PHYSICAL REVIEW B VOLUME 19, NUMBER 12 15 JUNE 1979

Cohesive properties of metallic compounds: Augmented-spherical-wave calculations

A. R. Williams and J. Kübler*
IBM Thomas J. Watson Research Center, Yorktown Heights, New York 10598

C. D. Gelatt, Jr.
Physics Department, Harvard University, Cambridge, Massachusetts 02138
(Received 25 September 1978)

We present a conceptual model and calculational procedure for the study of the electronic structure of metallic compounds. The model consists of spherical atoms compressed into finite volumes appropriate to the solid. The model involves no adjustable or experimentally derived parameters. All contributions to the total energy (other than the Madelung energy) are obtained from independent compressed-atom calculations. Interatomic interactions enter the calculations through the electronic configuration (the distribution of the valence charge among s, p, d, etc., states) and boundary conditions which give the atomic valence levels a finite width. These environmental constraints, which specify the state of the compressed atoms, are obtained from energy-band calculations. For the latter we introduce a new method, which we call the augmented-spherical-wave (ASW) method to stress its conceptual similarity to Slater's augmented-plane-wave (APW) method. The ASW method is a direct descendant of the linear-muffin-tin-orbitals technique introduced by Andersen; when applied to pure metals, it yields results which closely approximate those of the much more elaborate Korringa-Kohn-Rostoker calculations of Moruzzi, Williams, and Janak. The combined ASW compressed-atom procedure is tested on (i) the empty lattice, (ii) the pure metals Na, Al, Cu, and Mo, and (iii) the ordered stoichiometric compounds NaCl, NiAl, and CuZn. Finally, we demonstrate the utility of the procedure by using it to study the anomalous tendency of Ni and Pd (as compared to their Periodic Table neighbors Co, Cu, Rh, and Ag) to form hydride phases. We have calculated the total energies of the six pure metals and their monohydrides. The total energy differences exhibit the anomaly and an analysis of quantities internal to the calculation reveals its origin.

I. INTRODUCTION

This paper represents a contribution to the continuing effort to interpret the properties of condensed matter in terms of the properties of the atomic constituents. Recently there has been much activity in the development of empirical correlations between properties of solid compounds and those of either the free-atom[1-3] or pure-metal[4,5] constitutents. The work presented here is complementary to the empirical approach; our calculations require only the atomic number(s) as input, and the connection with bonding properties is utterly explicit. This explicitness is, however, both an advantage and a disadvantage: since our model exhibits bonding properties similar to those of real solids, it certainly contains the ingredients required for the simple intuitive picture of bonding that are sought by both approaches. Unfortunately, the elaborate computational link between input and output mixes, in a frequently obscure way, ingredients which are crucial with those which are less important. With these advantages and disadvantages in mind we have endeavored here to structure the nonempirical calculation of binding properties so as to cleanly separate intra- and interatomic contributions. We have additionally tried to "narrow the interface" between the intra- and interatomic parts of the calculation, that is, to condense into as compact a form as possible the information exchanged between the intra- and interatomic aspects of the calculation as the total process is iterated to self-consistency.

This work would not have been contemplated were it not for two recent developments in the theory of metals. First, it was shown[6] that a newly developed general theory of electronic structure, the local-density approximation,[7] provides a sufficiently accurate description of electronic exchange and correlation to permit the totally nonempirical calculation of metallic binding properties (equilibrium lattice constant, cohesive energy, and compressibility). Second, an approximate calculational scheme was proposed by Andersen[8] which, if sufficiently accurate, would make feasible for a wide range of metallic compounds calculations of the type performed for pure metals in Ref. 6.

The paper is organized as follows: Section II describes the formalism we have developed for the analysis of metallic binding. Section II A discusses the physical considerations which lead to the formalism. Sections II B, II C, and II D describe our treatment of the interatomic aspects of the problem. Sections II E and II F describe the construction of the electron density and the calculation of the total energy and the hydrostatic pressure; this develop-

ment builds on the work of Pettifor.[9] Section III describes the results obtained when the formalism is applied to systems for which the results are in some sense known. The applications discussed in Sec. III extend from the purely mathematical "empty-lattice" test through studies of pure transition, simple and noble metals, where the results can be compared to both experiment and previous calculations. Section III concludes with a study of the cohesive properties of compounds chosen to represent different types of bonding; here, the only comparison available is with experiment. Unlike Section III, where our objective is the creation of a body of evidence intended to provide an empirical indication of the accuracy of our methodology, Sec. IV provides an example of the type of analysis for which the methodology was developed. In Sec. IV we attempt to answer the question: Why do Ni and Pd form hydride phases, while their Periodic Table neighbors (Co, Cu, Rh, and Ag) do not? We first demonstrate that our mathematical model exhibits the same behavior seen in measurements on the real materials (which are unfortunately disordered and nonstoichiometric). We then look "inside" the model to identify the physical origin of the anomalous behavior of Ni and Pd. Finally, in Sec. V we offer our conclusions regarding the overriding question: Can such *ab initio* calculations play a useful role in the search for simple intuitive ways of understanding the cohesive properties of complicated and often not well-characterized systems?

II. CALCULATIONAL FORMALISM—AUGMENTED-SPHERICAL-WAVE METHOD

A. Physical considerations underlying our approach

As the introduction indicates, one of our basic objectives in this work is the separation of intra- and interatomic aspects of metallic cohesion. In Secs. II B–II D we are concerned with the interatomic aspects, the way in which the properties of the individual atomic constituents are coupled. The constituent atoms are, of course coupled by the wave (Schrödinger) equation; the electronic states of condensed matter are not confined to individual atoms; in general, they extend throughout the entire system. We shall see, however, that a different point of view is possible: We synthesize the true, extended states out of states that are locally atomic in character. The occupation of the extended states according to the rules of Fermi statistics implies the occupation (in general fractional) of the states associated with individual atoms. In this way we are led to the notion of an atom as it exists in a condensed phase.

As we shall see, the atom as it exists in a solid requires rather little information for its specification. The question naturally arises: Must we perform an elaborate energy-band calculation in order to obtain this limited information? This question has been answered in several ways by different authors. Even the need for a wave-mechanical coupling between the atoms has been challenged by a series of authors, who have attempted to obtain the required environmental information from Thomas-Fermi-like theories.[5, 10, 11] In this approach, the interatomic interaction between atomic cores, which are described wave mechanically, is mediated by an electron gas, which is described non-wave-mechanically.

This type of procedure is still being developed, and the limits of its applicability and accuracy are not known at this time. We have opted against this approach in the present work, because it is difficult so see on the basis of existing work how several important effects of an apparent interatomic origin are not lost in such treatments; we have in mind, e.g., level broadening, covalent interactions and the connection between the chemical environment of a given atom (crystal structure, e.g.) and its electronic configuration (the distribution of valence electrons among s, p, d, etc. states). The connection between crystal structure and electronic configuration is the basis of the Engel-Brewer theory of crystal phases[12]; if our theory is to provide any theoretical insight into such empirical correlations the wave-mechanical coupling of atoms must be retained in some form.

There are other alternatives to the full-blown band-theoretical treatment of the interatomic coupling. For example, Pettifor[9] uses an assumption of nearly-free-electron behavior for non-d electrons together with a canonical-band[8] description of the d-electrons to obtain the required specification of the atom in the solid. Much has been learned[9, 13] from these assumed forms for the electronic configuration and, in particular, its volume dependence, but a physical effect is ignored in such treatments, which is known[14, 15] to make a significant contribution to cohesive energies, namely the quantum-mechanical mixing of d states and non-d states or s-d hybridization.[16] We have therefore opted for a treatment of the interatomic aspect of the problem which is more elaborate than that given by canonical band concepts.

Energy-band calculations represent a large computational effort, particularly when compared with the limited amount of information we extract from them for the calculation of cohesive properties (see Secs. II E and II F), and we remain hopeful that

an alternative to them will be found. We feel, however, that there is presently no alternative which meets our needs in this regard and proceed now to a description of the procedure we have developed for efficiently performing the band-theoretic interatomic coupling.

B. Energy-independent basis sets and core orthogonality

The objective of the augmented-spherical-wave (ASW) method is the approximate, but efficient, determination of the eigenfunctions $\Psi(\vec{r},\epsilon)$ and the eigenenergies ϵ (in Ry) of the single-particle Schrödinger equation

$$[-\nabla^2+V(\vec{r})-\epsilon]\Psi(\vec{r},\epsilon)=0\ . \tag{1}$$

The density-functional approach to electronic-structure problems[7] requires the repeated solution of such equations as part of a self-consistent-field procedure. (The effective-one-electron potential $V(\vec{r})$ is defined in Sec. II F). The objectives of the analysis in Secs. II C, II D, and II E are: (i) the subdivision of the total calculation into intra- and interatomic parts and (ii) an efficient means of performing the latter.

The approach we take to these objectives incorporates two basic features. First, it is well known that the solution of equations of the form of Eq. (1) is greatly facilitated if the energy dependence of the solutions $\Psi(\vec{r},\epsilon)$ can be described by energy-dependent coefficients in an expansion of $\Psi(\vec{r},\epsilon)$ in a basis set of energy-independent functions $X_n(\vec{r})$, i.e.,

$$\Psi(\vec{r},\epsilon)=\sum_n C_n(\epsilon)X_n(\vec{r})\ . \tag{2}$$

The expansion of $\Psi(\vec{r},\epsilon)$ in ϵ-independent basis functions reduces the solution of the Schrödinger equation [Eq. (1)] to a matrix eigenvalue problem, for which efficient numerical procedures exist.

The second fundamental feature of our approach concerns the basis set $\{X_n(\vec{r})\}$ and can be described by contrasting our procedure with the traditional LCAO (linear combination of atomic orbitals) method. In the LCAO method, orbitals corresponding to atomic-core states are included in the basis set. This serves two purposes, (i) the orthogonalization of orbitals associated with a given atom to those corresponding to the core states of other atoms, and (ii) the description of changes in the core states caused by the presence of nearby atoms.[17] One of the central themes of the present development is that intra- and interatomic aspects of the calculation can be decoupled and that, in particular, both the required orthogonalization[8] and the core-state readjustments can be effected without the inclusion of core states in the basis set used to expand the extended states constituting the interatomic interaction. The elimination of core states from the (interatomic) basis set represents a substantial gain in efficiency; it is, for example, one of the fundamental sources of the greater efficiency of the scattered-wave method for molecules[18] over LCAO methods. To summarize, interatomic interactions involve (directly[19]) only the relatively narrow energy range and annular spatial shell which correspond to a single value of the atomic principal quantum number (the single value can be different for different angular momenta, as in transition metals); we exploit this fact by constructing a restricted basis set which spans the special set of functions in which we are interested.

C. Augmented spherical waves

Augmented spherical waves (ASW's) are the choice we make for the energy-independent, single-principal-quantum-number basis set just discussed. Their definition and construction reflect the qualitatively different types of behavior exhibited by the wave function $\Psi(\vec{r},\epsilon)$ in the intra- and interatomic portions of a polyatomic system. In the intra-atomic regions the strong effective potential causes $\Psi(\vec{r},\epsilon)$ to vary rapidly, whereas the interatomic region is characterized by a weak effective potential and slowly varying wave functions. These aspects of the interatomic region might be taken to argue for an expansion of the interatomic portion of $\Psi(\vec{r},\epsilon)$ in plane waves. [It is this reasoning that leads to Slater's augmented-plane-wave (APW) method.] Plane waves, however, treat all portions of the interstitial volume equally, a luxury for which the price is relative inefficiency. We opt here for a less flexible, and therefore less accurate, LCAO-like treatment of the interatomic region. In this region, we assume solutions of Schrödinger's equation to be a linear combination of atomic-orbital "tails" which extend out of each intra-atomic region. We therefore write

$$\Psi(\vec{r},\epsilon)=\sum_{L\nu} C_{L\nu}(\epsilon)H_L(\vec{r}-\vec{R}_\nu)\ , \tag{3}$$

where the $\{\vec{R}_\nu\}$ are nuclear positions and the $C_{L\nu}(\epsilon)$ are the energy-dependent expansion coefficients mentioned above. As individual atomiclike functions $H_L(\vec{r})$, we postulate spherical waves,

$$H_L(\vec{r})\equiv i^l\kappa^{l+1}Y_L(\hat{r})h_l^+(\kappa r), \tag{4}$$

where L is a composite index indicating both the angular-momentum quantum number l and the magnetic quantum number m; $Y_L(\hat{r})$ is a spherical

harmonic[20] and $h_l^+(x)$ is the outgoing spherical Hankel function.[20] [We remind the reader that the singular behavior of $h_l^+(\kappa r)$ for small r is irrelevant since we use the spherical waves only outside the intra-atomic (small r) regions.] The kinetic-energy parameter κ controls the localization of the basis-set orbital. In this paper it will be taken to be common to all orbitals and it will not be used as a variational parameter[21]; we therefore suppress it notationally. Our atomiclike functions $H_L(\vec{r})$ are postulated in the same intuitive spirit that Slater-type orbitals or Gaussian functions are postulated in many implementations of the LCAO method. The motivation for our particular choice of "atomic" functions is that they are particularly well adapted to the augmentation procedure, which we shall now describe.

In contrast to the interatomic region, each intra-atomic region is characterized by a very strong effective potential. For valence orbitals the large negative potential energy is cancelled by a correspondingly large kinetic energy. This delicate cancellation of large kinetic and potential energies argues for a careful numerical construction of solutions in this region. This would require a large numerical effort[22] were it not for the approximate spherical symmetry of the effective potential in this region. The assumption of spherical symmetry allows us to construct basis functions for this region by solving an ordinary (i.e., one-dimensional) differential equation, the radial Schrödinger equation; without this assumption we would be obliged to solve a partial (i.e., three-dimensional) differential equation. The way in which slowly varying spherical waves are combined with intra-atomic radial functions to form augmented spherical waves (ASW's) is shown schematically in Fig. 1. For reader's familiar with Slater's APW method, Fig. 1 also contains for comparison a schematic description of an (energy-independent[23]) APW. Figure 1 indicates that APW's and ASW's are very similar; the principal difference is that a single ASW, like an atomic orbital, is identified with a particular atom.

The mathematics of the augmentation process is straightforward. The spherical wave $H_L(\vec{r})$ is continued into the intra-atomic region by the particular linear combination[24] of solutions to the radial Schrödinger equation which joins smoothly to $H_L(\vec{r})$ at the interface of the intra- and inter-atomic regions. [While the intra-atomic region could in general have a complicated, (e.g., polyhedral) shape, for simplicity we take it to be spherical and centered on the nucleus.] For all $r_\nu(\vec{r}_\nu \equiv \vec{r} - \vec{R}_\nu)$ less than the sphere radius S_ν we replace $H_L(\vec{r}_\nu)$ by its augmented counterpart $\tilde{H}_L(\vec{r}_\nu)$

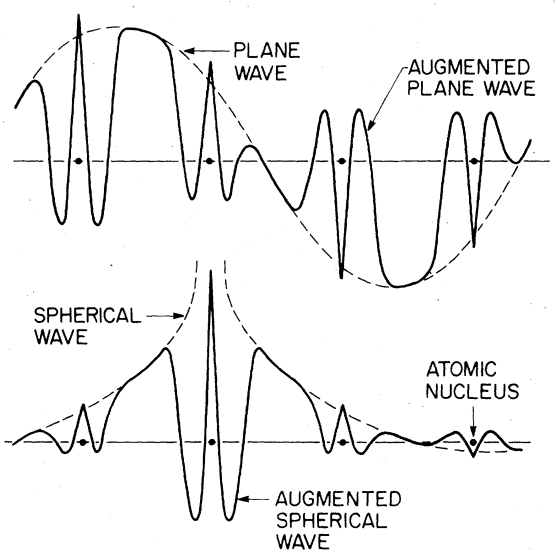

FIG. 1. Comparison of augmented plane and spherical waves. Both are energy independent and in both cases solutions of the radial Schrödinger equation, whose energy and normalization are chosen to provide continuous value and slope, replace the "unaugmented" wave in the intra-atomic region surrounding each nucleus.

(we use the tilde to denote augmentation), where

$$\tilde{H}_L(\vec{r}_\nu) \equiv i^l Y_L(\hat{r}_\nu)\tilde{h}_l(r_\nu), \tag{5}$$

and $\tilde{H}_L(\vec{r}_\nu)$ is a solution of the intra-atomic Schrödinger equation,

$$[-\nabla^2 + V(\vec{r}_\nu + \vec{R}_\nu) - \epsilon_{l\nu}^{(H)}]\,\tilde{H}_L(\vec{r}_\nu) = 0\ , \tag{6}$$

or equivalently

$$\left(-\frac{1}{r_\nu}\frac{d^2}{dr_\nu^2}\,r_\nu + \frac{l(l+1)}{r_\nu^2} + V(\vec{r}_\nu + \vec{R}_\nu) - \epsilon_{l\nu}^{(H)}\right)\tilde{h}_l(r_\nu) = 0\ , \tag{7}$$

and $V(\vec{r}_\nu + \vec{R}_\nu)$ is assumed to depend only on r_ν (for $r_\nu < S_\nu$). (The site at which the augmented Hankel function is centered will be indicated by the subscript on its argument.) The two degrees of freedom available in constructing $\tilde{h}_l(r_\nu)$, its normalization and the energy $\epsilon_{l\nu}^{(H)}$, are chosen so that $\tilde{H}_L(\vec{r}_\nu)$ is continuous and differentiable across the spherical surface $r_\nu = S_\nu$, i.e.,

$$\left(\frac{d}{dr_\nu}\right)^n [\tilde{h}_l(r_\nu) - \kappa^{l+1}h_l^+(\kappa r_\nu)]_{r_\nu = S_\nu} = 0; \quad n = 0, 1. \tag{8}$$

As mentioned above, the effective potential varies strongly in all the intra-atomic regions; we must therefore augment $H_L(\vec{r}_\nu)$ not only inside the sphere centered at $\vec{R}_\nu$, but in all other intra-atomic regions as well. This process is greatly facilitated

by the fact that $H_L(\vec{r}_v)$ can be represented in the vicinity of $\vec{R}_{v'}$ ($\neq \vec{R}_v$) by an expansion in Bessel functions $J_L(\vec{r}_{v'})$

$$H_L(\vec{r}_v) = \sum_{L'} J_{L'}(\vec{r}_{v'}) B_{L'L}(\vec{R}_{v'} - \vec{R}_v) , \tag{9}$$

where

$$J_L(\vec{r}) = i^l \kappa^{-l} Y_L(\hat{r}) j_l(\kappa r) \tag{10}$$

and $j_l(\kappa r)$ is a spherical Bessel function.[20] The expansion coefficients $B_{LL'}(\vec{R})$ are the structure constants which arise in the Korringa-Kohn-Rostoker (KKR) method of energy-band calculation[25] and the analogous scattered-wave method for molecules,[18]

$$B_{LL'}(\vec{R}) = 4\pi \sum_{L''} I_{LL'L''} \kappa^{l+l'-l''} H_{L''}(\vec{R}) \tag{11}$$

and

$$I_{LL'L''} \equiv \int d\hat{r}\, Y_L(\hat{r}) Y_{L'}(\hat{r}) Y_{L''}(\hat{r}) . \tag{12}$$

The augmentation of $H_L(\vec{r}_v)$ in the vicinity of $\vec{R}_{v'}$ therefore reduces to the augmentation of the spherical Bessel function $j_l(\kappa r_{v'})$, i.e., for $|\vec{r} - \vec{R}_{v'}| \leq S_{v'}$,

$$\tilde{H}_L(\vec{r} - \vec{R}_v) = \sum_{L'} \tilde{J}_{L'}(\vec{r} - \vec{R}_{v'}) B_{L'L}(\vec{R}_{v'} - \vec{R}_v) \tag{13}$$

where

$$\tilde{J}_L(\vec{r}_{v'}) \equiv i^l Y_L(\hat{r}_{v'}) \tilde{j}_l(r_{v'})$$

and $\tilde{j}_l(r_{v'})$ is the solution of the radial Schrödinger equation appropriate to the sphere centered at $R_{v'}$

$$\left(-\frac{1}{r_{v'}}\frac{d^2}{dr_{v'}^2} r_{v'} + \frac{l(l+1)}{r_{v'}^2} + V(\vec{r}_{v'} + \vec{R}_{v'}) - \epsilon_{lv'}^{(J)}\right) \times \tilde{j}_l(r_{v'}) = 0 \tag{14}$$

that joins the spherical Bessel function $j_l(\kappa r_{v'})$ smoothly,

$$\left(\frac{d}{dr_{v'}}\right)^n [\tilde{j}_l(r_{v'}) - \kappa^{-l} j_l(\kappa r_{v'})]_{r_{v'} = s_{v'}} = 0; \quad n = 0, 1, \tag{15}$$

at $r_{v'} = S_{v'}$. As with the augmentation of $h_l^+(\kappa r)$, the continuity conditions [(Eq. (15)] specify the normalization of $\tilde{j}_l(r_{v'})$ and the energy $\epsilon_{lv'}^{(J)}$. Note that $\tilde{h}_l(r_v)$ and $\tilde{j}_l(r_v)$ are solutions of the same radial Schrödinger equation; they differ only in normalization and energy. The four functions $h_l^+(\kappa r)$, $\tilde{h}_l(r)$, $j_l(\kappa r)$, and $\tilde{j}_l(r)$ are compared in Fig. 2. [The fact that the augmentation of spherical waves introduces two energies and the corresponding radial wave functions provides a superficial and potentially misleading similarity to the procedure of Ref. 8, where two functions (a radial wave function and its energy derivative) are also used to represent $\epsilon_{lv}^{(H)}$ and $\epsilon_{lv'}^{(J)}$. The difference between augmentation and the procedure of Ref. 8 is more evident when other functions, such as Gaussians or Slater functions, are augmented, for in such cases not two but many energies are introduced. The distinction is particularly clear in the case of plane waves whose augmentation introduces a continuous set of such energies and radial wave functions. All of these energies *can* be represented using an energy Taylor series, but *augmentation and the approximately linear energy dependence of radial wave functions are*

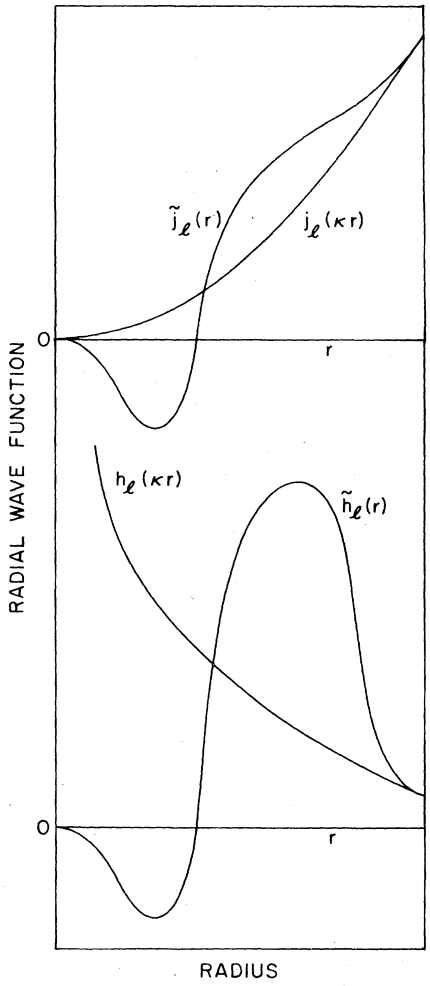

FIG. 2. Schematic diagram comparing the spherical Bessel functions $h_l^+(\kappa r)$ and $j_l(\kappa r)$ and their augmented counterparts $\tilde{h}_l(r)$ and $\tilde{j}_l(r)$. The curves shown correspond to $l = 2$. Note that $\tilde{h}_l(r)$ and $\tilde{j}_l(r)$ are solutions to the same radial Schrödinger equation; they differ in energy and normalization.

completely independent concepts. Note also that the angular momentum and site dependence of the energies and radial wave functions introduced by augmentation provide an additional (with respect to the procedure of Ref. 8) adaptation of the basis set to the valence electronic structure of *each* constituent atom.[26]]

Our augmented spherical waves $\{\tilde{H}_L(\vec{r}-\vec{R}_\nu)\}$ are now defined in all regions of the polyatomic system; they are energy independent, continuous, and continuously differentiable. We feel that they constitute an efficient set of basis functions in which to expand solutions of Schrödinger's equation; Eq. (2) becomes

$$\Psi(\vec{r},\epsilon)=\sum_{L,\nu} C_{L\nu}(\epsilon)\tilde{H}_L(\vec{r}-\vec{R}_\nu)\ . \tag{16}$$

Note further that the ASW's involve only a single value of the principal quantum number index for each angular momentum. The particular choice of principal quantum number is made when the conditions Eqs. (8) and (15) are imposed. These conditions are satisfied by, not a single value of $\epsilon_{l\nu}^{(H)}$ and $\epsilon_{l\nu'}^{(J)}$ but a set of values—one for each principal quantum number. We use only the one value corresponding to the valence state of interest and the core oscillations naturally introduced into $\tilde{h}_l(r)$ and $\tilde{j}_l(r)$ during the integration of the radial equations [Eqs. (7) and (14)] guarantee that each of our ASW's is essentially orthogonal to *all* the core states of the polyatomic system.

D. Hamiltonian and overlap matrix elements in the ASW basis set

In Sec. II C we described the construction of individual members of the ASW basis set; in this section we describe the evaluation of the Hamiltonian $\mathcal{H}$ and normalization matrix elements required by the Rayleigh-Ritz variational procedure for the determination of the eigenenergy ϵ and the expansion coefficients $C_{L\nu}(\epsilon)$ appearing in the ASW expansion of the wave function [Eq. (16)]. The secular matrix given by the Rayleigh-Ritz procedure is simply

$$\sum_{L',\nu'}(\langle\nu\tilde{L}|\mathcal{H}|\tilde{L}'\nu'\rangle-\epsilon\langle\nu\tilde{L}|\tilde{L}'\nu'\rangle)C_{L'\nu'}(\epsilon)=0\ , \tag{17}$$

where $\mathcal{H}\equiv-\nabla^2+V(\vec{r})$ and $\langle\cdots|\cdots\rangle$ indicates integration over all space, e.g.,

$$\langle\nu\tilde{L}|\tilde{L}'\nu'\rangle\equiv\int d^3r\,\tilde{H}_L^*(\vec{r}-\vec{R}_\nu)\tilde{H}_{L'}(\vec{r}-\vec{R}_{\nu'})\ . \tag{18}$$

We eliminate the interstitial region by taking the intra-atomic regions to be space-filling polyhedra and approximate the individual polyhedra by spheres (the Wigner-Seitz or atomic-sphere approximation). This approximation can be used[8] to justify writing the matrix elements as a sum over contributions from each atomic sphere,

$$\langle\nu\tilde{L}|\mathcal{H}|\tilde{L}'\nu'\rangle=\sum_{\nu''}\langle\nu\tilde{L}|\mathcal{H}|\tilde{L}'\nu'\rangle_{\nu''}\ , \tag{19}$$

where $\langle\cdots|\cdots\rangle_{\nu''}$ indicates integration over the sphere centered at $\vec{R}_{\nu''}$, but we proceed differently. Taking the effective potential to be zero in the interstitial region (which we are free to do if we later eliminate the interstitial region) allows us to write the matrix elements as follows

$$\begin{aligned}\langle\nu\tilde{L}|\mathcal{H}|\tilde{L}'\nu'\rangle=&\langle\nu L|\mathcal{H}_0|L'\nu'\rangle\\&+\sum_{\nu''}(\langle\nu\tilde{L}|\mathcal{H}|\tilde{L}'\nu'\rangle_{\nu''}\\&-\langle\nu L|\mathcal{H}_0|L'\nu'\rangle_{\nu''})\ ,\end{aligned} \tag{20}$$

where $\mathcal{H}_0(\equiv-\nabla^2)$ denotes the free-particle Hamiltonian. In other words, we first construct matrix elements of $\mathcal{H}_0$ using *un*augmented spherical waves and integrating over all space; we then replace the contributions to this integration from the intra-atomic regions by integrations over the full Hamiltonian and ASW's. The motivation for this manipulation is that the integrations over the atomic spheres are performed using spherical-harmonic expansions and the expansion of the difference in parentheses in Eq. (20) converges much more rapidly than does the corresponding expansion of $\langle\nu\tilde{L}|\mathcal{H}|\tilde{L}'\nu'\rangle_{\nu''}$ alone. This improved l convergence represents not only a gain in efficiency, but a gain in accuracy as well.[27] The gain in accuracy is discussed below (Sec. II E) in connection with the construction of the electron density.

The final steps in the specification of the Hamiltonian matrix elements consist of exploiting the fact that, in all the integrals required by our representation of the matrix elements [Eq. (20)], the ASW is an eigenfunction of the relevant Hamiltonian. For example,

$$\langle\nu L|\mathcal{H}_0|L'\nu'\rangle=\kappa^2\langle\nu L|L'\nu'\rangle\ . \tag{21}$$

The integrals over the atomic spheres which appear in Eq. (20) are of three basic types, one-center, two-center, or three-center, depending on how many of the two ASW's involved are centered in the sphere over which the integration is being performed. One-center contributions are those in which both ASW's are centered in the sphere; in the notation of Eq. (20), $\nu=\nu'=\nu''$. In this case only augmented Hankel functions enter:

$$\langle\nu\tilde{L}|\mathcal{H}|\tilde{L}'\nu\rangle_\nu=\epsilon_{l\nu}^{(H)}\langle\tilde{H}_L|\tilde{H}_L\rangle_\nu\delta_{LL'}\ . \tag{22}$$

Two-center contributions ($\nu=\nu''\neq\nu'$ or $\nu\neq\nu''=\nu'$)

require the structure-constant expansion of one of the two ASW's, so that both augmented Bessel functions and augmented Hankel functions enter:

$$\langle \nu'' \tilde{L} | \mathcal{H} | \tilde{L}' \nu' \rangle_{\nu''} = \epsilon^{(J)}_{l\nu''} \langle \tilde{H}_L | \tilde{J}_L \rangle_{\nu''} B_{LL'}(\vec{R}_{\nu''} - \vec{R}_{\nu'}) \quad (23a)$$

$$\langle \nu \tilde{L} | \mathcal{H} | \tilde{L}' \nu'' \rangle_{\nu''} = B^{\dagger}_{LL'}(\vec{R}_{\nu} - \vec{R}_{\nu''}) \langle \tilde{J}_{L'} | \tilde{H}_{L'} \rangle_{\nu''} \epsilon^{(H)}_{l'\nu''} , \quad (23b)$$

where

$$B^{\dagger}_{LL'}(\vec{R}_{\nu} - \vec{R}_{\nu'}) \equiv B^{*}_{L'L}(\vec{R}_{\nu'} - \vec{R}_{\nu}).$$

Three-center contributions arise when neither of the two ASW's involved in the matrix element are centered in the intra-atomic region over which the integration is being performed ($\nu \neq \nu' \neq \nu''$); in this case two structure-constant expansions are required (one for each ASW) and only augmented Bessel functions enter the final integration

$$\langle \nu \tilde{L} | \mathcal{H} | \tilde{L}' \nu' \rangle_{\nu''} = \sum_{L''} B^{\dagger}_{LL''}(\vec{R}_{\nu} - \vec{R}_{\nu''}) \epsilon^{(J)}_{l''\nu''} \times \langle \tilde{J}_{L''} | \tilde{J}_{L''} \rangle_{\nu''} B_{L''L'}(\vec{R}_{\nu''} - \vec{R}_{\nu'}) . \quad (24)$$

The representation (20) of the matrix elements requires an integral over all space involving unaugmented spherical waves; fortunately, such integrals can be performed analytically. Integrals of this kind in which both spherical waves have a common center are simply

$$\langle \nu L | L' \nu \rangle - \langle \nu L | L' \nu \rangle_{\nu} = \delta_{LL'} \langle H_L | H_L \rangle'_{\nu} , \quad (25)$$

where $\langle \cdots | \cdots \rangle'_{\nu}$ refers to integration over all of space *except* the interior of the atomic sphere centered at $\vec{R}_{\nu}$, e.g.,

$$\langle H_L | H_{L'} \rangle'_{\nu} \equiv \kappa^{2l+2} \int_{S_{\nu}}^{\infty} r_{\nu}^2 \, dr_{\nu} |h_l^{+}(\kappa r_{\nu})|^2 . \quad (26)$$

[Note that the integral $\langle \nu L | L' \nu \rangle_{\nu}$, which in general is singular, subtracts out of the formula (20) for the matrix element.] The normalization integral involving spherical waves centered at different nuclei, i.e., $\langle \nu L | L' \nu' \rangle$ with $\nu \neq \nu'$, is given by the energy derivative of the corresponding structure constant,

$$\langle \nu L | L' \nu' \rangle = \dot{B}_{LL'}(\vec{R}_{\nu} - \vec{R}_{\nu'}) = \frac{d}{d\kappa^2} B_{LL'}(\vec{R}_{\nu} - \vec{R}_{\nu'}) . \quad (27)$$

[Note that the κ^2 dependence of $H_L(\vec{r})$ and $B_{LL'}(\vec{R})$, which has been suppressed notationally, is exhibited explicitly in Eqs. (4) and (11).] Equation (27) is obtained by differentiating the free-particle Schrödinger equation satisfied by $H_L(\vec{r})$ with respect to κ^2 and by using the result

$$(\nabla^2 + \kappa^2) \dot{H}_{L'}(\vec{r} - \vec{R}_{\nu'}) + H_{L'}(\vec{r} - \vec{R}_{\nu'}) = 0 \quad (28)$$

to express $\langle \nu L | L' \nu' \rangle$ as the integral over infinitesimal spherical surfaces[28] enclosing the singularities in the integral at $\vec{R}_{\nu}$ and $\vec{R}_{\nu'}$; the surface integrals are then evaluated (trivially) using the structure-constant expansion [Eq. (13)].

The expressions for the individual integrals which enter our representation (20) for the Hamiltonian matrix elements, i.e., Eqs. (21)–(27), can now be combined to complete the specification of the secular matrix:

$$\begin{aligned}\langle \nu L | \mathcal{H} | L' \nu' \rangle = {} & [\epsilon^{(H)}_{l\nu} \langle \tilde{H}_L | \tilde{H}_L \rangle_{\nu} + \kappa^2 \langle H_L | H_L \rangle'_{\nu}] \delta_{LL'} \delta_{\nu\nu'} + \kappa^2 \dot{B}_{LL'}(\vec{\tau}_{\nu} - \vec{\tau}_{\nu'}, \vec{k}) \\ & + B^{\dagger}_{LL'}(\vec{\tau}_{\nu} - \vec{\tau}_{\nu'}, \vec{k}) [\epsilon^{(H)}_{l'\nu'} \langle \tilde{J}_{L'} | \tilde{H}_{L'} \rangle_{\nu'} - \kappa^2 \langle J_{L'} | H_{L'} \rangle_{\nu'}] \\ & + [\epsilon^{(J)}_{l\nu} \langle \tilde{H}_L | \tilde{J}_L \rangle_{\nu} - \kappa^2 \langle H_L | J_L \rangle_{\nu}] B_{LL'}(\vec{\tau}_{\nu} - \vec{\tau}_{\nu'}, \vec{k}) \\ & + \sum_{\nu''} \sum_{L''} B^{\dagger}_{LL''}(\vec{\tau}_{\nu} - \vec{\tau}_{\nu''}, \vec{k}) [\epsilon^{(J)}_{l''\nu''} \langle \tilde{J}_{L''} | \tilde{J}_{L''} \rangle_{\nu''} \\ & - \kappa^2 \langle J_{L''} | J_{L''} \rangle_{\nu''}] B_{L''L'}(\vec{\tau}_{\nu''} - \vec{\tau}_{\nu'}, \vec{k}) , \end{aligned} \quad (29)$$

where translational symmetry has been exploited by introducing the structure constants[29] appropriate to energy-band theory,

$$B_{LL'}(\vec{\tau}, \vec{k}) \equiv \sum_{\vec{R}} e^{+i\vec{k}\cdot\vec{R}} B_{LL'}(\vec{\tau} + \vec{R}) , \quad (30)$$

where $B_{LL'}(\vec{x})$ is defined to be zero when $\vec{x}$ vanishes, the $\vec{R}$'s constitute a Bravais lattice, and the $\vec{\tau}$'s indicate the positions of the atoms within the unit cell. The normalization matrix is obtained from Eq. (29) by setting the energies κ^2, $\epsilon^{(J)}_{l\nu}$, and $\epsilon^{(H)}_{l\nu}$ equal to unity. A simple manipulation of

Eqs. (7) and (14) shows that $\langle \tilde{H}_L | \tilde{J}_L \rangle_\nu = \langle \tilde{J}_L | \tilde{H}_L \rangle_\nu = (\epsilon_{l\nu}^{(H)} - \epsilon_{l\nu}^{(J)})^{-1}$, so that, like Andersen's,[8] our secular matrix involves only four problem-dependent quantities (for each l and ν), $\epsilon_{l\nu}^{(H)}, \epsilon_{l\nu}^{(J)}$, $\langle \tilde{H}_L | \tilde{H}_L \rangle_\nu$, and $\langle \tilde{J}_L | \tilde{J}_L \rangle_\nu$. The required integrals involving augmented functions require only one-dimensional (radial) numerical integrations and those involving unaugmented spherical Bessel functions can be found in Morse and Feshbach.[30] The largest angular momenta used in both the secular matrix and in the internal L'' summation[31] [the three-center contribution to Eq. (29)] are discussed in Sec. III, which deals with test applications of the method. [While Eq. (29) does not exhibit the Hermiticity of the Hamiltonian and normalization matrices explicitly, this important property is in fact guaranteed by the continuous differentiability of each trial orbital. (Continuous differentiability permits the integrations by parts required to formally demonstrate Hermiticity.)]

One of the attractive features of an LCAO-like method such as ours is the interpretability of the matrix elements. We identify the site-diagonal terms with atomic quantities, the terms involving one B and the mixed integrals $\langle \tilde{H}_L | \tilde{J}_L \rangle_\nu$ and $\langle \tilde{J}_L | \tilde{H}_L \rangle_\nu$ with two-center-contributions. The augmentation procedure can be viewed as accomplishing a "pseudization" of the interatomic interaction in an LCAO basis similar to that obtained by Anderson.[32] In other words, the augmentation procedure automatically accounts for the effective weakening of the intra-atomic potential by the valence kinetic energy. The net result, as can be seen directly in Eq. (29), is the representation of the interatomic interaction in terms of valence energies ($\epsilon_{l\nu}^{(J)}$ and $\epsilon_{l\nu}^{(H)}$), which are seldom larger than a few electron volts. It should be noted, however, that while the *form* of the ASW secular matrix is LCAO-like, the interatomic interactions are *not* confined to near neighbors. Our successful description of free-electronlike materials, such as aluminum, (applications are described in Sec. III) requires the inclusion of long-range interactions. In this respect our results are consistent with those of Chadi,[33] who showed that the empirical-pseudopotential description of the energy bands of Si (a procedure involving a large secular matrix when the pseudo-wave-function is expanded in plane waves) can be essentially duplicated by a much smaller LCAO secular matrix, provided that long-range interactions and orbital overlap are properly included. It should also be noted in this context that, when the spherical-wave kinetic energy κ^2 is taken to be positive, our "atomic-orbital-like" spherical waves are normalizable only in the δ-function sense that plane waves are normalizable, i.e., the integral in Eq. (26) does not exist. As a result, a slightly different derivation of the secular matrix is required when $\kappa^2 > 0$. The modified derivation is given in the Appendix. Fortunately, only minor details of the secular matrix change in the $\kappa^2 > 0$ case.

E. Construction of the electron density

Self-consistent calculations such as those we discuss in the Secs. III and IV require explicit construction of the electron density. The approximation responsible for the great numerical efficiency of the ASW and linear-muffin-tin-orbitals (LMTO)[8] techniques introduce ambiguities intc this process. In this section we discuss these ambiguities and describe a procedure for constructing the electron density which exploits the strengths of the ASW method and minimizes the effects of its weaknesses.

The weaknesses in question are of two basic types: (i) the nonvariational character of the wave function provided by the Rayleigh-Ritz procedure in combination with the restricted energy-independent basis set and (ii) the overlap of the atomic (or Wigner-Seitz) spheres. The Rayleigh-Ritz procedure is fundamentally a least-squares procedure; it provides an accurate representation of only those aspects of the wave function that are important to the energy functional. Thus, for example, the spherical-harmonic decomposition of a particular Rayleigh-Reitz eigensolution $\Psi(\vec{r}, \epsilon^{(k)})$ implies l-dependent radial functions that are individually a linear combination of augmented Bessel and Hankel functions. Each such linear combination corresponds to an l-dependent orbital eigenenergy $\epsilon_l^{(k)}$. In determinantal methods (APW and KKR, e.g.) these eigenenergies $\{\epsilon_l^{(k)}\}$ are all equal to one another and to the eigenenergy $\epsilon^{(k)}$ of the solution as a whole; the secular equation in such methods can be viewed as the algebraic statement that all these energies must be equal. Rayleigh-Ritz solutions are different; the $\epsilon_l^{(k)}$ are not equal to one another or to $\epsilon^{(k)}$. The situation is typical of least-squares procedures; if the eigensolution $\Psi(\vec{r}, \epsilon^{(k)})$ is dominated by a particular value of l, such as a d state then $\epsilon_l^{(k)}$ for that l will closely approximate $\epsilon^{(k)}$, but in general the other $\epsilon_l^{(k)}$ will differ considerably.

Because of these problems with Rayleigh-Ritz wave functions, we have elected *not* to use them directly in constructing the electron density, but rather to emphasize the role of the most reliable aspect of the Rayleigh-Ritz procedure, the variationally determined eigenenergies $\epsilon^{(k)}$. To do this we take the electron density to have the form it *would* have in a more accurate KKR or APW calculation, i.e.,

$$\rho_\nu(r_\nu)=\rho_\nu^{(c)}(r_\nu)+\sum_l \int^{\epsilon_f} d\epsilon\, \rho_{l\nu}(\epsilon)R_{l\nu}^2(r_\nu,\epsilon)\ , \quad (31)$$

where $\rho_\nu(r_\nu)$ is the spherical average of the electron density in the νth atomic sphere; $\rho_\nu^{(c)}(r_\nu)$ is the contribution of the core levels; $R_{l\nu}(r_\nu,\epsilon)$ is a normalized solution of the radial Schrödinger equation appropriate to the νth sphere; $\rho_{l\nu}(\epsilon)$ is the valence-electron state density decomposed according to angular momentum and atomic site, and the energy integration extends over the occupied valence bands.

Our procedure for constructing the electron density is not yet completely specified, for although it is clear that the *total* valence state density $\rho(\epsilon)$,

$$\rho(\epsilon)=\sum_{l\nu}\rho_{l\nu}(\epsilon)=\sum_k \delta(\epsilon-\epsilon^{(k)})\ , \quad (32)$$

requires only a knowledge of the eigenenergies $\epsilon^{(k)}$, the *partial* state densities $\rho_{l\nu}(\epsilon)$ appearing in our representation of the electron density (Eq. 31) require the decomposition of the norm of each eigenstate $\Psi(\vec{r},\epsilon^{(k)})$, i.e.,

$$\rho_{l\nu}(\epsilon)=\sum_k \delta(\epsilon-\epsilon^{(k)})q_{l\nu}^{(k)}\ , \quad (33)$$

where the $q_{l\nu}^{(k)}$ are the l and ν decomposition of the single electron norm associated with each eigenstate ($\sum_{l\nu}q_{l\nu}^{(k)}\equiv 1$. It might seem therefore that the representation of the electron density in terms of partial state densities merely exchanges one problem for another, i.e., the l and ν decomposition of each eigenstate requires wave-function information which is given somewhat unreliably by the Rayleigh-Ritz procedure. The advantage of the present method of constructing the electron density is that is exploits the fact that the normalization of a radial wave function varies more slowly with energy than the wave function itself.[34]

The required decomposition of the normalization of each state could be obtained straightforwardly, were it not for the second of the two weaknesses mentioned at the beginning of this section, the overlap of the atomic spheres and the associated problem of the convergence of spherical-harmonic expansions. Fortunately, our procedure for constructing the matrix elements [Eq. (20)] provides a degree of control over both of these problems. The integral constituting each matrix element is performed by first integrating the unaugmented functions over all of space and then integrating the augmentation contribution over the atomic spheres. The integration over the unaugmented functions is performed exactly and therefore involves neither the atomic-sphere overlap nor the convergence of angular-momentum expansions. The integration over the augmentation contribution involves both of these problems, but benefits from the fact that the augmentation contribution to the wave function vanishes quadratically on the atomic sphere. This means that the augmentation contribution to the normalization matrix is small *throughout* the overlap region, thereby reducing the overlap problem, and also that it is small at large radii, thereby improving the l convergence.[35] The normalization of each eigenstate by the requirement

$$\sum_{L\nu}\sum_{L'\nu'} C_{L\nu}^{(k)*}\langle \nu\tilde{L}\,|\,\tilde{L}'\nu'\rangle C_{L'\nu'}^{(k)}=1 \quad (34)$$

is therefore a particularly reliable aspect of the calculation and one we want to emphasize in constructing the electron density. Setting all the energies appearing in Eq. (29) to unity provides an explicit expression for the normalization matrix $\langle \nu\tilde{L}\,|\,\tilde{L}'\nu'\rangle$, which when substituted into Eq. (34) allows the normalization to be written as a single summation over atomic sites and angular momenta *plus a small quantity* $\delta^{(k)}$.

$$\begin{aligned}1=\sum_{L\nu}(&C_{L\nu}^{(k)*}\langle\tilde{H}_L\,|\,\tilde{H}_L\rangle_\nu C_{L\nu}^{(k)}+C_{L\nu}^{(k)*}\langle\tilde{H}_L\,|\,\tilde{J}_L\rangle_\nu A_{L\nu}^{(k)}\\&+A_{L\nu}^{(k)*}\langle\tilde{J}_L\,|\,\tilde{H}_L\rangle_\nu C_{L\nu}^{(k)}\\&+A_{L\nu}^{(k)*}\langle\tilde{J}_L\,|\,\tilde{J}_L\rangle_\nu A_{L\nu}^{(k)})+\delta^{(k)}\ , \end{aligned} \quad (35)$$

where the coefficient $A_{L\nu}^{(k)}$ of the augmented Bessel function is given by

$$A_{L\nu}^{(k)}\equiv\sum_{L'\nu'} B_{LL'}(\vec{\tau}_\nu-\vec{\tau}_{\nu'},\vec{k})C_{L'\nu'}^{(k)}\ . \quad (36)$$

Thus, if it were not for the quantity $\delta^{(k)}$, Eq. (35) would constitute the required ν and l decomposition of the normalization. [The decomposition according to l is obtained from the L decomposition by summing over m; $L\equiv(l,m)$.]

The significance of the quantity $\delta^{(k)}$ is that it would vanish identically if there were no atomic-sphere overlap and if the spherical-harmonic expansions were completely converged; $\delta^{(k)}$ is the (exactly computed) contribution to the normalization due to unaugmented spherical waves minus the integral over the atomic spheres of the spherical-harmonic expansion of the *same quantity*. Since both of the factors leading to nonzero $\delta^{(k)}$ are associated with large values of l, we have elected to combine the contribution $\delta^{(k)}$ to the normalization with the contribution corresponding to the largest value of l used in each atomic sphere.[36] With $\delta^{(k)}$ absorbed into the fourth term, Eq. (35) provides the required normalization decomposition $q_{l\nu}^{(k)}$, which together with Eqs. (31) and (32), completely specifies the electron density.

Our representation of the electron density [Eq. (31)], together with the fact that the energy de-

pendence of solutions to the radial Schrödinger equation is approximately linear,[8] suggests a further simplification. Equation (31) shows that if the ϵ dependence of the radial wave functions were perfectly linear, then the electron density $\rho_\nu(r)$ would rigorously depend on only the first three moments of the (occupied) partial state densities $\rho_{l\nu}(\epsilon)$. While the radial wave functions are not perfectly linear in energy, their near linearity suggests that a representation of the electron density based on the first *four* partial-state-density moments is probably adequate. We are thus lead to the following compact representation of the electron density

$$\rho_\nu(r) = \rho_\nu^{(\mathrm{core})}(r) + \sum_l \sum_{i=1,2} Q_{l\nu}^{(i)} R_{l\nu}^2(r, \epsilon_{l\nu}^{(i)}), \tag{37}$$

where the two charges $Q_{l\nu}^{(i)}$ and the two energies $\epsilon_{l\nu}^{(i)}$ (for each l and ν) are determined by the requirement that this representation [Eq. (37)] of the electron density preserve the first four moments of *each* partial state density, i.e.,

$$\sum_{i=1,2} Q_{l\nu}^{(i)} \left(\epsilon_{l\nu}^{(i)}\right)^n = \int^{\epsilon_F} d\epsilon\, \rho_{l\nu}(\epsilon)\epsilon^n, \quad n = 0, 1, 2, 3. \tag{38}$$

Having transformed the interatomic information provided by the energy-band calculation from partial state densities to moments and from moments to the charges $Q_{l\nu}^{(i)}$ and energies $\epsilon_{l\nu}^{(i)}$, one additional transformation of the information contained in the energies $\epsilon_{l\nu}^{(i)}$ will complete the specification of our procedure for constructing the electron density. We prefer to think of the environment of a given atom as characterized by boundary conditions which the intra-atomic wave functions are obliged to satisfy. The effective one-electron potential and the radial Schrödinger equation containing it imply an unambiguous relationship between the energy $\epsilon_{l\nu}^{(i)}$ and the logarithmic derivative $D_{l\nu}^{(i)}$ of the corresponding solution at the surface of the atomic sphere, i.e.,

$$D_{l\nu}^{(i)} \equiv [rR_{l\nu}(r, \epsilon)]^{-1} \frac{d}{dr} R_{l\nu}(r, \epsilon), \quad r = S_\nu, \ \epsilon = \epsilon_{l\nu}^{(i)}, \tag{39}$$

where S_ν is the radius of the νth atomic sphere. This characterization of the environment in terms of electronic configurations $\{Q_{l\nu}^{(i)}\}$ and boundary conditions $\{D_{l\nu}^{(i)}\}$ imposed at finite radii $\{S_\nu\}$ provides a link with intuitive theories of metallic bonding and crystal structure. The basis of the theory of metallic cohesion due to Wigner and Seitz[37] is the difference between atomic boundary conditions and those characteristic of a partially filled energy band. The analysis of crystal-structure preference due to Engel and Brewer[12] is based exclusively on electronic configurations, i.e., the $Q_{l\nu}$ ($\equiv \sum_{i=1,2} Q_{l\nu}^{(i)}$). Finite-volume atoms in environment-determined configurations constitute the concept underlying the "renormalized-atom" theory of metals.[14] The contribution of the present analysis is the establishment of a rigorous link between these intuitively appealing concepts and *ab initio* self-consistent-field calculations. This link has already been successfully exploited in the analysis of core-level binding-energy shifts observed in x-ray photoemission electron spectroscopy for chemical analysis (ESCA),[38] where, more than any other single quantity, the electronic configuration $Q_{l\nu}$ determines the variation of the binding-energy shift with atomic number.

The characterization of the atom in terms of the charges $Q_{l\nu}^{(i)}$ and the boundary conditions $D_{l\nu}^{(i)}$ also has the practical virtue of decoupling intra- and interatomic self-consistency. In other words, once the $Q_{l\nu}^{(i)}$ and $D_{l\nu}^{(i)}$ have been produced by a band calculation, the atomic calculation they specify can be iterated to self-consistency before another band calculation is performed. In this way every band calculation performed in the course of obtaining interatomic self-consistency is based on atomic potentials which are internally self-consistent. This fact substantially reduces the number of band calculations required for total self-consistency. Recent work by Zunger and Freeman[39] exploits the same basic idea.

F. Intra-atomic calculations—total energy and hydrostatic pressure

In the preceding subsections of Sec. II we showed how the ASW formulation of the energy-band problem permits the interatomic aspects of the electronic structure to be described as a process which, when given four numbers characterizing each atomic valence level $\{\epsilon_{l\nu}^{(i)}, \langle \tilde{I}_L | \tilde{I}_L \rangle_\nu; \ I = J, \ H\}$, produces four new quantities $\{D_{l\nu}^{(i)}, \ Q_{l\nu}^{(i)}; \ i = 1, 2\}$ which characterize the contribution of each orbital to the electron density of the polyatomic system. In this section we show that this characterization of the electron density implies expressions for the total energy and hydrostatic pressure which are desirable in that they allow these quantities to be decomposed in intuitive ways. For example, the total energy is represented as the sum of individual compressed-atom total energies plus a Madelung contribution.

Consider first the total energy E as given by the density-functional formalism,[6,7]

$$E = T_S + U + E_{xc}, \tag{40}$$

where T_S is the kinetic energy of a system of noninteracting electrons possessing the same electron density as the system in question,

$$T_S \equiv \sum_k \int d^3r\, \Psi_k^*(\vec{r})(-\nabla^2)\Psi_k(\vec{r}), \quad \epsilon^{(k)} \leq \epsilon_f; \tag{41}$$

the electrostatic energy U is the sum of electron-electron-nucleus, and nucleus-nucleus contributions

$$U \equiv \int d^3r\, \rho(\vec{r}) \int d^3r'\, \rho(\vec{r}')\left|\vec{r}-\vec{r}'\right|^{-1} - 2\int d^3r\, \rho(\vec{r}) \sum_\nu Z_\nu \left|\vec{r}-\vec{R}_\nu\right|^{-1} + \sum_\nu Z_\nu \sum_{\nu' \neq \nu} Z_{\nu'} \left|\vec{R}_\nu - \vec{R}_{\nu'}\right|^{-1}, \tag{42}$$

where Z_ν is the atomic number of the atom centered at $\vec{R}_\nu$. (Note that our use of Rydbergs as the energy unit implies somewhat nonintuitive coefficients for ∇^2 in T_S and the three contributions to the electrostatic energy U.) The quantity E_{xc} is the contribution of exchange and correlation, to which we make the local-density approximation,[7] i.e.,

$$E_{xc} \approx \int d^3r\, \rho(\vec{r}) \epsilon_{xc}^h(n)\big|_{n=\rho(\vec{r})} \tag{43}$$

where $\epsilon_{xc}^h(n)$ is the contribution per electron to the total energy of an interacting, but homogeneous, electron gas of density n. The orbitals $\Psi_k(\vec{r})$ appearing in Eq. (41) are those whose squares constitute the electron density $\rho(\vec{r})$, i.e.,

$$\rho(\vec{r}) \equiv \sum_k \left|\Psi_k(\vec{r})\right|^2, \quad \epsilon^{(k)} \leq \epsilon_f. \tag{44}$$

Minimization of the total energy E by the variation of the orbitals $\Psi_k(\vec{r})$ leads to Schrödinger-like Euler equations for the $\Psi_k(\vec{r})$

$$[-\nabla^2 + V(\vec{r}) - \epsilon^{(k)}]\Psi_k(\vec{r}) = 0 \tag{45}$$

in which the effective-one-electron potential $V(\vec{r})$ is the sum of electron-electron and electron-nucleus electrostatic terms plus a contribution due to exchange and correlation

$$V(\vec{r}) = 2\int d^3r'\, \rho(\vec{r}')\left|\vec{r}-\vec{r}'\right|^{-1} - 2\sum_\nu Z_\nu \left|\vec{r}-\vec{R}_\nu\right|^{-1} + \frac{d}{dn} n\epsilon_{xc}^h(n)\big|_{n=\rho(\vec{r})}. \tag{46}$$

The fact that the $\Psi_k(\vec{r})$ entering the total-energy expression [Eq. (40)] satisfy the Schrödinger equation [Eq. (45)] can be used to express the total energy as the sum of the orbital eigenenergies $\epsilon^{(k)}$ plus the nuclear electrostatic energy and so-called two-electron or "double-counting" terms

$$E = \sum_k \epsilon^{(k)} + \sum_\nu Z_\nu \sum_{\nu' \neq \nu} Z_{\nu'} \left|\vec{R}_\nu - \vec{R}_{\nu'}\right|^{-1} - \int d^3r\, \rho(\vec{r})\Big\{n\frac{d}{dn}\epsilon_{xc}^h(n)\big|_{n=\rho(\vec{r})} + \int d^3r_1\, \rho(\vec{r}_1)\left|\vec{r}-\vec{r}_1\right|^{-1}\Big\}. \tag{47}$$

(The k summation includes only occupied states.) It is into this form for the total energy that we shall introduce our particular representation of the electron density, i.e., that given by self-consistent compressed-atom calculations specified by the boundary conditions $D_{l\nu}^{(i)}$ and corresponding charges $Q_{l\nu}^{(i)}$ $(i=1,2)$.

Our objective is to rewrite the total-energy expression [Eq. (47)] as a sum of similar expressions for each of the compressed atoms E_ν^A plus a Madelung contribution E^M, i.e.,

$$E = \sum_\nu E_\nu^A + E^M, \tag{48}$$

where E^M is the electrostatic energy associated with the lattice of ions

$$E^M \equiv \sum_\nu (Q_\nu - Z_\nu) \sum_{\nu' \neq \nu} (Q_{\nu'} - Z_{\nu'})\left|\vec{R}_\nu - \vec{R}_{\nu'}\right|^{-1}. \tag{49}$$

The quantities Q_ν and Z_ν are, respectively, the electronic and nuclear charges associated with the νth atomic sphere; Q_ν is simply the sum of the orbital charges introduced in Sec. II E plus the charges $Q_\nu^{(c)}$ associated with core states,

$$Q_\nu \equiv \sum_l \sum_{i=1,2} Q_{l\nu}^{(i)} + \sum_c Q_\nu^{(c)}. \tag{50}$$

For single-constituent systems (e.g., pure metals) $Q_\nu = Z_\nu$ and the Madelung energy E^M is zero (in the atomic-sphere approximation).

To effect this decomposition of the total energy we must recognize that in rewriting the total energy in terms of one-electron energies $\epsilon^{(k)}$ we have implicitly taken as a reference energy the zero of the electrostatic, or Hartree, potential, i.e., the effective potential given in Eq. (46) without the exchange-correlation contribution. It is therefore not surprising that, when the compressed-atom total energies E_ν^A are expressed in the form of Eq. (47), the one-electron energies which appear must be referred to the zero of the *local* Hartree potential $V_\nu^H(r)$. The latter is the electrostatic potential due only to charges in the particular atomic sphere, i.e.,

$$V_\nu^H(r) \equiv -2\left(\frac{Z_\nu}{r} - \int_0^{S_\nu} dr_1\, 4\pi r_1^2 \rho_\nu(r_1)\frac{1}{r_>}\right), \tag{51}$$

where $r_>$ is the larger of r and r_1 and S_ν is the radius of the νth atomic sphere. The local reference energies are introduced into the total-energy expression [Eq. (47)] by adding and subtracting the quantity $\sum_\nu Q_\nu \phi_\nu^M$, where ϕ_ν^M is the Madelung potential in each atomic sphere,

$$\phi_\nu^M = 2 \sum_{\nu' \neq \nu} (Q_{\nu'} - Z_{\nu'}) |\vec{R}_\nu - \vec{R}_{\nu'}|^{-1}. \tag{52}$$

The Madelung potential ϕ_ν^M relates the local reference energies to one another and to the global Hartree potential. Combining the subtracted $\sum_\nu Q_\nu \phi_\nu^M$ with the sum of one-electron energies appearing in Eq. (47) introduces the effective valence-orbital energies ($\epsilon_{l\nu}^{(i)}$; $i=1,2$) discussed in Sec. IIE, i.e.,

$$\sum_k \epsilon^{(k)} - \sum_\nu Q_\nu \phi_\nu^M = \sum_{l\nu} \sum_{i=1,2} \bar{\epsilon}_{l\nu}^{(i)} Q_{l\nu}^{(i)} + \sum_{c\nu} \bar{\epsilon}_\nu^{(c)} Q_\nu^{(c)}, \tag{53}$$

where the "bar" on the local core and valence orbital eigenenergies $\bar{\epsilon}_\nu^{(c)}$ and $\bar{\epsilon}_{l\nu}^{(i)}$ indicates that they are referred to the zero of the local Hartree potential, i.e., $\bar{\epsilon}_{l\nu}^{(i)} \equiv \epsilon_{l\nu}^{(i)} - \phi_\nu^M$. The valence energies $\bar{\epsilon}_{l\nu}^{(i)}$ are those implied by the boundary conditions (logarithmic derivatives) $D_{l\nu}^{(i)}$, which in turn are specified by the partial state densities given by the energy-band calculation (see Sec. IID). This relationship [Eq. (53)] says nothing more than, if the reference energy in the νth sphere is changed by ϕ_ν^M, then the total energy associated with shifting the energies of Q_ν electrons by this amount must be accounted for. When the $\sum_\nu Q_\nu \phi_\nu^M$, which we have added to the total-energy expression [Eq. (47)], is combined with the nuclear-nuclear electrostatic energy and the interatomic portion of the electron-electron "double-counting" integral

$$-\int d^3r\, \rho(\vec{r}) \int d^3r_1\, \rho(\vec{r}_1) |\vec{r} - \vec{r}_1|^{-1},$$

we obtain the Madelung energy [Eq. (49)] and the desired expression for the constituent atomic energies,

$$E_\nu^A \equiv \sum_l \sum_{i=1,2} Q_{l\nu}^{(i)} \bar{\epsilon}_{l\nu}^{(i)} + \sum_c Q_\nu^{(c)} \bar{\epsilon}_\nu^{(c)} - \int_0^{S_\nu} dr\, 4\pi r^2 \rho_\nu(r) \times \left(n \frac{d\epsilon_{xc}^h}{dn}\Big|_{n=\rho_\nu(r)} + \int_0^{S_\nu} dr_1\, 4\pi \rho_\nu(r_1) r_>^{-1} \right). \tag{54}$$

Equations (48), (49), and (54) constitute the desired total-energy decomposition. It should be noted that such a decomposition is only possible when both the electron density and the effective one-electron potential are taken to be spherically symmetric in each atomic sphere, for only in this case do charges outside a given sphere have the limited effect of simply shifting all energies in the sphere by a constant Madelung potential [Eq. (52)].

We turn now to the evaluation of the hydrostatic pressure. Since the motivation for calculating the pressure can be seen and stated more concisely once the algebraic form of the pressure expression has been presented, we momentarily defer such discussion and proceed with the derivation. We begin by differentiating our site-decomposed expression for the total energy, [Eq. (48)],

$$3P\Omega = -a\frac{dE}{da} = -\sum_\nu S_\nu \frac{dE_\nu}{dS_\nu} - a\frac{dE^M}{da}, \tag{55}$$

where P is the internal pressure (positive if the total energy decreases with expansion), Ω is the volume of the unit cell, and a is the lattice constant. Expressions for the pressure have been given by Liberman,[40] by Janak,[41] and, most recently, by Pettifor,[9] who presented an expression for $S_\nu\, dE_\nu^A/dS_\nu$ appropriate to the local-density theory of exchange; the inclusion of correlation (as suggested by Pettifor) leads to the following result,

$$S_\nu \frac{dE_\nu^A}{dS_\nu} = \sum_l \sum_{i=1,2} Q_{l\nu}^{(i)} 4\pi r^3 [R_{l\nu}^{(i)}(r)]^2 \times \left\{ [D_{l\nu}^{(i)}(D_{l\nu}^{(i)}+1) - l(l+1)](1/r^2) + \bar{\epsilon}_{l\nu}^{(i)} - V_\nu(r) + n\frac{d\epsilon_{xc}^h}{dn}\Big|_{n=\rho_\nu(r)} \right\}, \tag{56}$$

where $R_{l\nu}^{(i)}(r)$ and $\bar{\epsilon}_{l\nu}^{(i)}$ are the (normalized) radial solution and orbital eigenenergy implied by the boundary condition $D_{l\nu}^{(i)}$ (see Sec. IIE), and r is to be evaluated at the sphere radius S_ν. The effective potential V_ν appearing in Eq. (56) is the local Hartree potential defined in Eq. (51) plus the contribution of exchange and correlation [the last term in Eq. (46)]. The explicit dependence of the Madelung energy E^M on the lattice constant a is trivial,

$$-a\frac{\partial E^M}{\partial a} = E^M, \tag{57}$$

so that Eqs. (55), (56), and (57) complete the specification of the pressure. Before going on, we note two subtleties in the derivation of the pressure expression. First, one can neglect the implicit dependence of the Madelung energy E^M on the lattice constant a through the a dependence of the site charges Q_ν, because of the stationarity of the total energy with respect to variations in

the electron density, i.e.,

$$\frac{dE}{da}=\frac{\partial E}{\partial a}+\int d^3r\frac{d\rho(\vec{r})}{da}\frac{\delta E}{\delta\rho(\vec{r})}. \tag{58}$$

The fact that, for any value of a, we determine the electron density to minimize the total energy E guarantees that $\delta E/\delta\rho(\vec{r})$ vanishes. Second, Eq. (56) can only be obtained algebraically (i.e., without appeal to scaling arguments) from Eq. (54) if it is assumed that the lattice-constant dependence of the distribution of boundary conditions makes no contribution to the pressure. We *believe*[42] that this assumption is in fact justified.

Evaluation of the hydrostatic pressure is useful in a number of ways. From a purely practical point of view, it facilitates determination of the equilibrium lattice constant, because it passes linearly through zero at equilibrium, in constrast to the total energy, which passes through a quadratic minimum.[43] More importantly, the pressure provides a valuable tool for studying the site and angular-momentum decomposition of binding.[9,14,44] This is not merely the statement that Eq. (56) consists of a sum over ν and l; the pressure provides a decomposition of binding which is intuitively satisfying. In particular, it involves only states which have significant amplitude on the surface of the atomic sphere.[45] To appreciate these virtues of the pressure, it must be compared with other quantities used to analyze binding. The sum of the one-electron energies is frequently used, but it suffers the disadvantage of ignoring other contributions to the total energy[14,6,46] and of involving an arbitrary reference energy. For example, the surface dipole-layer potential[47] shifts the one-electron energies of a solid relative to those of the free atom[38] and yet plays no role in cohesion, because the energy gained in adding an additional atom to a solid involves moving a *neutral* atom through the surface potential, not merely a collection of electrons.[48] A quantity which is not "fooled" in this way by such potential-energy changes is the kinetic energy T. The latter has the virtue of being state decomposable and unambiguously related to binding by the virial theorem.

$$E=3P\Omega-T. \tag{59}$$

The total-energy difference δE between two equilibrium ($P=0$) configurations is therefore the negative of the change in kinetic energy δT,

$$\delta E=-\delta T. \tag{60}$$

The difficulty encountered when using the kinetic energy to analyze binding is that changes in T are not confined to valence states. Thus, for example, when binding in transition metals is analyzed according to Eq. (60), one finds that the upper core levels (the $3p$ levels in the $3d$-transition series) are "responsible for cohesion."[49] This statement is not wrong; it merely indicates that the kinetic-energy analysis does not provide an intuitively satisfying interpretation of binding. The interpretation provided by analysis of the pressure suffers none of these drawbacks.

Evaluation of the pressure has another practical virtue; the virial-theorem-based expression for the total energy given in Eq. (59) is an independent alternative to those given earlier in this section, and as such provides an invaluable check on our numerical procedures. Perfect agreement between the total energies given by Eqs. (59) and (47) requires the exact solution of both Poisson's equation and Schrödinger's equation in each sphere. Agreement does not indicate the elimination of systematic errors such as those introduced by our use of the local-density and atomic-sphere approximations, or by our neglect of relativistic effects, but it does indicate the elimination of random errors and it is these which would most corrupt the small total-energy *differences* of interest in our attempts to interpret metallic binding. Thus, for example, Eq. (47) yields an energy of $-35\,720.9668$ Ry for fcc gold, whereas Eq. (59) yields $-35\,720.9671$ Ry. Both of these energies contain systematic errors much larger than the energy differences of interest, but their agreement indicates that the *random* error in the total-energy differences discussed in Secs. III and IV is probably smaller than 0.01 eV.

It should be noted that the kinetic energy T appearing in Eq. (59) is not merely the expectation value of the operator $-\nabla^2$ described by T_S [Eq. (41)], but includes the kinetic-energy contribution T_{xc} of the exchange-correlation functional, i.e.,

$$T=T_S+T_{xc}. \tag{61}$$

In the local-density approximation T_{xc} is given by

$$T_{xc}\cong\int d^3r\,\rho(\vec{r})[3\frac{d}{dn}n\epsilon^h_{xc}(n)-4\epsilon^h_{xc}(n)]_{n=\rho(\vec{r})}. \tag{62}$$

This relationship[50] follows from the fact that $\epsilon^h_{xc}(n)$ satisfies Eq. (59), i.e.,

$$\epsilon^h_{xc}(n)=-r_s\frac{d}{dr_s}\epsilon^h_{xc}(n)-t^h_{xc}(n), \tag{63}$$

where $\frac{4}{3}\pi r_s^3=n^{-1}$, and kinetic-energy density $t^h_{xc}(n)$ is the bracketed quantity in Eq. (62).

III. NUMERICAL TESTS

The ASW method we propose is based on three independent approximations: (i) the effective-one-electron potential is assumed to be spherically symmetric inside each of a set of volume-filling spheres; (ii) our LCAO-like basis set is always restricted and therefore not complete, and (iii) the energy dependence of the wave functions inside each sphere is represented by an energy-dependent linear combination of only two energy-independent functions. In this section we apply the method to problems with known solutions, where the meaning of the word known will vary considerably. We begin with the so-called empty lattice[51] for which all the individual eigenenergies and wave functions are known exactly; we next consider metals for which "known" means the existence of more accurate calculations and we conclude with a study of the prototypical compounds NaCl, NiAl, and CuZn for which "known" means only that reliable experimental measurements exist for the ordered, stoichiometric compounds.

A. Empty lattice and metallic elements

The results of the application of the ASW method to the empty lattice are compared with the exact band energies in Fig. 3. The lattice structure is face-centered cubic; the maximum angular momentum used[52] was 2 and the kinetic-energy parameter κ^2 describing the localization of the spherical waves was taken (everywhere in this paper) to be -0.01 Ry.[53] Figure 3 indicates that our ASW technique is most reliable for the low-energy states; fortunately, for the occupied states in metals (at most 3 mobile electrons per atom, or 1.5 nearly-free-electron bands) the method appears quite reliable even in a test as stringent as that posed by the empty lattice. This is born out by our calculations for Al. Figure 4 compares the energy bands given by the ASW procedure with those of the KKR method.[54] In the Al calculations, spherical waves corresponding to $l=0$, 1, and 2 were used and the internal l summation in the three-center contribution to the secular matrix (see Sec. II D) was extended to $l=3$.[55] The Al calculations constitute a stringent test of the method, not only because of the nearly-free-electron character of the states, but also because of the large occupied bandwidth, as well. Figure 4 exhibits an effect of the constant-κ approximation; the small value of κ used in the calculation is more appropriate to the bottom of the band than to the top, thereby artificially exagerating the bandwidth by the small amount visible in the figure. The Al calculations also test our procedure for constructing the electron density (see Sec. II E), i.e., the energy bands labelled ASW in Fig. 4 employ, not the potential used in the KKR calculations, but rather the self-consistent potential given by iteration of the ASW procedure to self-consistency.[56] This particular point is exhibited more directly in our test calculations for metallic copper. Table I contains band energies for three calculations: the KKR calculation,[54] the ASW calculation using the potential given by the KKR calculation, and the ASW calculation, itself iterated to self-consistency. Comparison of the first two sets of results indicates the accuracy of the ASW band methodology *per se*; comparison of the second and third probes the accuracy of our two-valence-state representation of the electron density (see Sec. II E), and comparison of the first and third probes the accuracy of the combined procedure.

The results presented in Figs. 3 and 4 and in Table I indicate that our approximations introduce small errors into individual band energies;

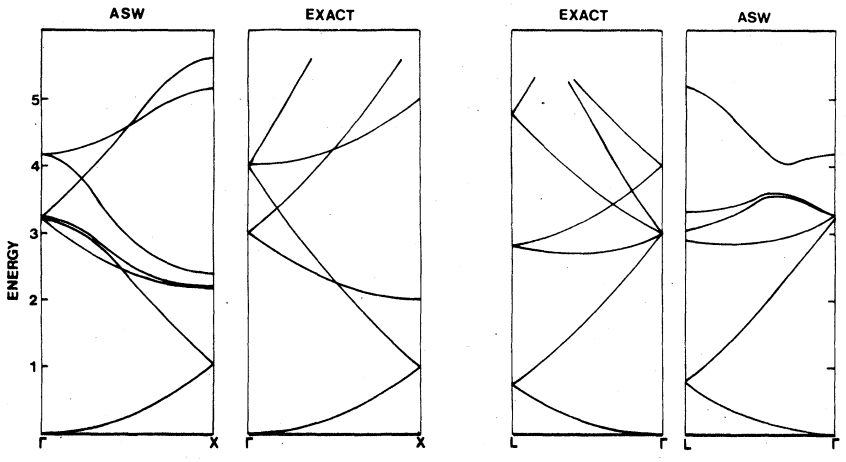

FIG. 3. Comparison of exact energy bands for the "empty lattice" with those given by the ASW method.

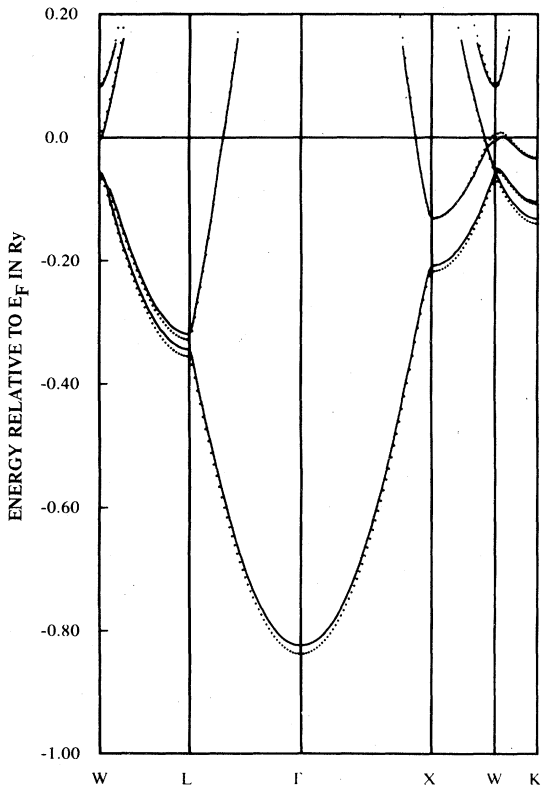

FIG. 4. Comparison of the energy bands of aluminum given by the KKR method (Ref. 54) with those given by the ASW method (dots) iterated to self-consistency. The lattice constant (7.60 bohr) is that which minimizes the total energy in both calculations (See Ref. 56).

we consider now the effects of these errors on the quantities of principal interest, the binding properties given by the total energy and pressure. Of interest to us are the three fundamental properties of the binding curve (total energy versus lattice constant), the position of the minimum (equilibrium lattice constant), the depth of the minimum[58] (cohesive energy) and the curvature near the minimum (bulk modulus or compressibility). Table II compares the results of our ASW calculations with those of KKR calculations[54] and with experiment.[59,60] Table II presents results for the monovalent metal K, the polyvalent metal Al, the transition metal Mo and the noble metal Cu. The evident success of the calculations is particularly encouraging in light of the complete absence of experimental input and the greatly reduced computational effort. (The ASW calculations require approximately 1% the computation required for the KKR results.)

B. Prototypical compounds: NaCl, NiAl, and CuZn

In this short section, we compare with experiment our calculated binding properties (lattice constant, heat of formation, and bulk modulus) for three compounds representing three different types of bonding. Rocksalt (NaCl) is a strongly bound ionic compound, CuZn is a weakly bound metallic compound, and NiAl represents a mixture of metallic and covalent[61] binding which results in bonding of intermediate strength. While there now exist several self-consistent band-

TABLE I. ASW-KKR comparison for Cu. Results of three energy-band calculations for fcc copper (lattice constant = 6.76 bohr).

Symmetry point	Energies (Ry)						
Γ	−0.064	0.390	0.390	0.390	0.451	0.451	a
	−0.067	0.391	0.391	0.391	0.452	0.452	b
	−0.082	0.389	0.389	0.389	0.451	0.451	c
X	0.241	0.284	0.494	0.509	0.509	0.748	a
	0.248	0.289	0.495	0.510	0.510	0.757	b
	0.242	0.285	0.494	0.509	0.509	0.742	c
L	0.242	0.386	0.386	0.497	0.497	0.544	a
	0.245	0.386	0.386	0.498	0.498	0.555	b
	0.239	0.384	0.384	0.497	0.497	0.537	c

[a] Self-consistent KKR results (Ref. 54).

[b] ASW results using potential generated by the KKR calculations.

[c] Self-consistent ASW results. Self-consistent energy-band calculations necessarily introduce an arbitrary reference energy [see Ref. (57)], which must be specified in order to compare the energies of the third calculation with those of the first two. In the tabulation above the Fermi energy of the third calculation was equated to that of the first (0.628).

TABLE II. Metallic-binding-property comparison. Comparison of calculated and experimental Wigner-Seitz radius, cohesive energy and bulk modulus. The three rows for each element give respectively the experimental values (Refs. 59 and 60), results of the present work, and results of KKR calculations (Refs. 6 and 54). Calculated cohesive energies include a small contribution due to zero-point vibrations (see Ref. 54).

		Wigner-Seitz radius (bohr)	Cohesive energy (Ry/atom)	Bulk modulus (Mbar)
Al	Expt	2.97	0.249	0.88
	ASW	2.97	0.295	0.87
	KKR	2.97	0.285	0.80
K	Expt	4.86	0.069	0.04
	ASW	4.71	0.069	0.05
	KKR	4.65	0.066	0.04
Cu	Expt	2.66	0.256	1.42
	ASW	2.66	0.298	1.29
	KKR	2.64	0.304	1.55
Mo	Expt	2.91	0.501	2.71
	ASW	2.95	0.494	2.68
	KKR	2.90	0.498	2.51

theoretical studies of compounds involving transition metals,[62] we believe that the calculations reported here are the first to deduce binding properties from a knowledge of only the relevant atomic numbers. (Our calculations also involve the choice of a lattice structure, but changes in binding properties with lattice structure are generally much smaller than the binding properties themselves.)

The numerical comparison provided by Table III indicates that our procedure[63] provides a reliable estimate of the binding energy of interest[64] in each case. This small set of results suggests that the error in our calculated binding energies is roughly 0.1 eV/atom. The fact that this error is similar in magnitude to that associated with our calculations of pure-metal cohesive energies is interesting, because it indicates that we are not profiting from an *additional* cancellation of errors when we subtract the pure-metal total energies from that corresponding to the compound. The important inference to draw from Table III is that we have constructed a model of compound formation which closely mirrors reality for a very broad class of materials. An advantage of the model over experimental reality is that the inner workings of the model are more amenable to study than are those of real systems. In other words, with the credibility of our model established and some idea of its limitations in hand, it now makes sense to look inside the model and try to understand in a detailed way why some compounds form, while others do not. Section IV describes our efforts to do this for a particularly interesting subset of the transition-metal hydrides.

TABLE III. Compound-binding-property comparison. Comparison of measured and calculated lattice constants, heats of formation, and bulk moduli. The contribution of magnetic order to the total energy of pure Ni was obtained from Ref. 54.

Compound		Lattice constant (bohr)	ΔH (eV/atom)	Bulk modulus (Mbar)
NaCl	Expt	10.7[a]	4.01[a]	0.26[b]
	ASW	10.2	4.05	0.32
NiAl	Expt	5.45[c]	0.61[d]	...
	ASW	5.44	0.74	1.7
CuZn	Expt	5.58[c]	0.12[d]	1.2[b]
	ASW	5.50	0.14	1.5

[a] Experimental data, Ref. 65.
[b] Experimental data, Ref. 60.
[c] Experimental data, Ref. 66.
[d] Experimental data, Ref. 67.

IV. PRINCIPAL FACTORS CONTROLLING THE ABILITY OF TRANSITION METALS TO FORM HYDRIDES

In contrast to all other sections of this paper which are concerned with the description of a new methodology and the calibration of its numerical accuracy, this section describes an example of the type of application for which the formalism was developed. The transition-metal hydrides are interesting systems about which a great deal remains to be understood. They seldom exist as stoichiometric ordered compounds and in some cases they do not exist at all (without the application of external pressure). We focus here on the question: Why do Ni and Pd form hydrides, while their Periodic Table neighbors Co, Cu, Rh, and Ag do not? Much has been learned about the electronic structure of metallic hydrides from the energy-band calculations of Switendick,[68] but no explanation is provided for the anomalous tendency of Ni and Pd to form hydrides. Gelatt *et al.*[69] have studied the energy of formation of hydrides of the 3*d*- and 4*d*-transition metals in an attempt to identify the important variables of the problem. Their conclusions are tentative in large part because of uncertainties introduced by approximations made in the course of the analysis. When the basic ideas of Ref. 69 are studied using the more accurate methodology described above, the following simple picture of hydride formation emerges. The interstitial hydrogen proton provides an attractive potential for the metal electrons. The lowering of the energy of those metal states with significant amplitude in the vicinity of the proton is the basic bonding mechanism; it results in a band of states that is often split off below the remaining energy bands of the system. This split-off hydride band leads to a separate peak in the state density of the hydrides which lies below the structure associated with the *d* electrons. This aspect of the state density is common to all the transition-metal hydrides; it can be seen in Fig. 5, where we compare our calculated state densities for pure metallic Co, Ni, Cu, Rh, Pd, and Ag with those of their monohydrides. Figure 5 shows, as did the calculations of Gelatt *et al.*, that the bonding caused by the interstitial proton, which is directly reflected in the amount by which the hydride band is split off below the *d* bands, decreases smoothly as we move toward the noble metal in each series. Thus, while the effect of the proton on the metallic electrons is the principal binding mechanism, the monotonic variation of this effect with atomic number cannot explain the anomalous tendency of Ni and Pd to form hydrides.

According to Gelatt *et al.*, while most of the

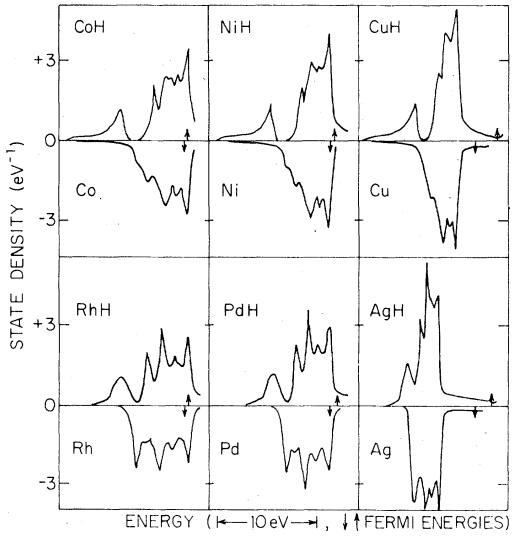

FIG. 5. State densities for six transition and noble metals and their NaCl-structure monohydrides. The state density due to the hydride band isolated below the *d*-band structure is clearly discernable in each hydride state density. The state density of the metal and its hydride were aligned in energy so that the peak due to localized states near the top of the *d* band falls at the same energy in the pure metal and the hydride. The arrows indicate the position of the Fermi energy in each case. The lattice constant in each case is that which minimizes the calculated total energy (see Table IV).

bonding is due to the proton, it is the electron of the hydrogen which leads to the interesting *variation* of the bonding with atomic number. The additional electron enters the system at the chemical potential of the metal and it is the variation of the latter which is responsible for the anomalous solubility of hydrogen in Ni and Pd. Estimates of the chemical potential of the transition-metal hosts[70] based on the renormalized-atom model[71] provided some support for the idea; the chemical potential, considered as a function of atomic number, decreased on moving from Fe to Co to Ni, but changed little on moving to Cu. When this variation of the energy associated with adding the electron is combined with the weakening binding energy of the proton just mentioned, an interpretation of the anomalous tendency of Ni and Pd to form hydrides is provided.

The present analysis supports this interpretation and our less approximate calculations clarify some of the internal arguments. First, our calculations show (in contrast to those of Ref. 69) that the chemical potential of the pure-metal host decreases *monotonically* on moving from Co to Ni to Cu and from Rh to Pd to Ag. *But*, the finite additional concentration of electrons provided by the hydrogen elevates the effective chemical po-

tential[72] in the noble metals, where the Fermi-level state density is small. As a result of this elevation, which is readily apparent in Fig. 5, the effective chemical potential, i.e., the energy associated with the addition of the electrons (of the hydrogen), exhibits a sharp minimum at Ni in the $3d$ series and at Pd in the $4d$ series. In our view it is this minimum which is responsible for the anomalous hydride formation in Ni and Pd. Figure 6 displays the evidence supporting this view. In Fig. 6(a) we compare our calculated heats of formation for ordered monohydrides with estimates inferred from measurements on nonstoichiometric samples; in Fig. 6(b) we show the variation of our calculated (effective) chemical potential. In assessing the information presented in Fig. 6 it should be born in mind that the variation we are concerned with is only a matter of a few tenths of an electron volt, which is at the limit of the accuracy of both the calculations[73] and the experiment. Nonetheless, the hydride calculations do exhibit the anomalous tendency of Ni and Pd to form hydrides, and Fig. 6(b) shows that the effective chemical potential exhibits a variation of similar shape and magnitude. Thus, our calculations lead to the same general conclusions[74] reached in Ref. 69 and, in our opinion, put them on a substantially more secure footing.

The accuracy with which equilibrium lattice constants for NaCl, NiAl, and CuZn are given by our procedure (see Sec. III B) suggests that our calculated dilatation of the metal lattic by hydrogen solution is reliable. Table IV presents the calculated equilibrium lattice constants for the six monohydrides and the experimental values for NiH_x and PdH_x. We find that the notion that hydrogen increases the volume of the unit cell by a constant amount is approximately correct; for the sequence Co, Ni, Cu, Rh, Pd, and Ag the effective Wigner-Seitz radius of the hydrogen is 1.6, 1.7, 1.7, 1.7, 1.7, and 1.8 Bohr. It is interesting that the heat of solution is most easily understood by considering the hydrogenic proton and electron separately, while the lattice dilitation is most easily understood in terms of the neutral atom.

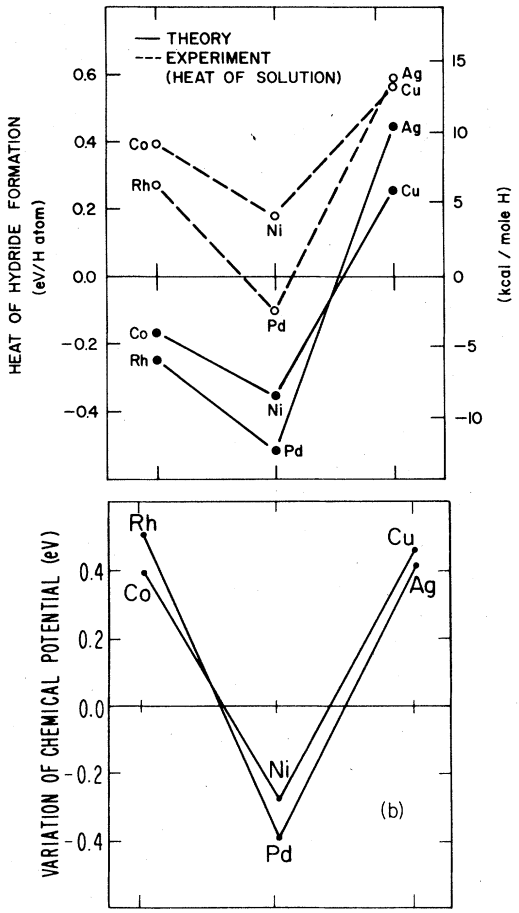

FIG. 6. Correlation of heat of hydride formation with effective chemical potential of metallic host. Comparison of our calculated heats of formation [E(hydride) $-E$(metal) $-\frac{1}{2}E(H_2$ molecule)] with experimental heats of hydrogen solution (Ref. 76). A more appropriate experimental comparison, possible only in the systems with a hydride phase, is the hydride heat of formation [1.2kcal/mole for NiH, -4.8 kcal/mole for PdH (Ref. 75)], which is in somewhat better agreement with the calculated values. (b) shows that the corresponding variation of the effective chemical potential is similar in shape and amplitude. The calculation of the total energy of the H_2 molecule is described in Ref. 77.

V. SUMMARY AND CONCLUSIONS

The objective of the present work is to demonstrate that parameter-free electronic-structure calculations can play a useful role in studying questions of interatomic binding which arise in the context of solid-state chemistry and metallurgy. The approach taken has been to identify the essential variables and to develop accurate but efficient computational procedures to describe the complex interactions among them.

Our work builds on that of Moruzzi *et al.*,[6,54] which demonstrates that metallic binding can be accurately described in the local-density approximation, and on that of Andersen,[8] who introduced a procedure for greatly improving the efficiency of the energy-band calculations required for the study of cohesive properties. We have shown that this procedure can be viewed as a particular synthesis of two ideas, that of energy-independent basis sets and the concept of augmentation due to Slater. We have combined these two ideas somewhat more directly into an accurate, yet intuitively

TABLE IV. Lattice dilatation resulting from Hydride formation. Comparison of calculated and measured lattice constants for pure metals and their hydrides. Measured values for NiH and PdH are data for nonstoichiometric hydrides (Ref. 75). Measured pure-metal lattice constants from Ref. 66.

Material	Calculated lattice constant (bohr)	Measured lattice constant (bohr)
Co	6.5	6.7
CoH	7.0	•••
Ni	6.6	6.7
NiH	7.1	7.01–7.06
Cu	6.8	6.8
CuH	7.3	•••
Rh	7.3	7.2
RhH	7.7	•••
Pd	7.4	7.4
PdH	7.9	7.81
Ag	7.8	7.7
AgH	8.32	•••

transparent, method of calculating the total-energy differences relevant to compound formation. In so doing we have condensed the gross quantity of information manipulated in *ab initio* electronic-structure calculations into those variables which characterize the atomic constituents and those which characterize the crystalline environment. Self-consistent-field calculations carried out in terms of this small set of variables accurately describe the bonding properties of representatives of both pure metals and a broad class of compounds.

More importantly, we feel that our analysis of hydride formation demonstrates that the ASW methodology can be helpful in developing simple ways of thinking about complicated systems. The ASW calculations play two roles in this context; they provide a type of very well-characterized data on which to build interpretive theories. In addition, however, we have tried to structure the calculation in terms of quantities amenable to interpretation, site, and orbital charges, etc. The example of hydride formation does not make extensive use of all the interpretive features of our model, atomic decompositions and hydrostatic pressure, for example; no single example will. As mentioned above, the analysis of core-level binding energies[38] exploited the self-consistent electronic configurations given by the model for transition metals. The pressure decomposition [Eq. (55)] provides the basis for an unpublished analysis of metallic binding; and an analysis of the strengths and limitations of non-wave-mechanical interpretations of compound formation[5,10,11] is under way which relies on the atomic decomposition of the total energy. We are encouraged by the model's utility thus far and we have high hopes that it will provide a useful link between microscopic and macroscopic descriptions of binding in a wide variety of systems.

ACKNOWLEDGMENTS

We gratefully acknowledge helpful discussions of this work with U. von Barth, N. D. Lang, and J. F. Janak. We also gratefully acknowledge the assistance of V. L. Moruzzi with regard to computer graphics. The initial discussions which led to this work took place during the Effective-one-electron-potential workshop at the Centre Europeen de Calcul Atomique et Moleculaire, Orsay, France. One of us (J.K.) would like to thank IBM World Trade Corp. for support under the visiting scientist program for the period of time during which this work was initiated. One of us (C.D.G.) is grateful to the IBM Thomas J. Watson Research Center for summer-faculty-visitor support and to the NSF under Grant No. DMR-77-10210 for partial support.

APPENDIX: ASW method for $\kappa^2 > 0$

This appendix serves two purposes: the basic purpose is to show how the secular matrix elements are constructed when the spherical waves are normalizable only in the δ-function sense, i.e., when $\kappa^2 > 0$; the secondary purpose is to provide some of the details of the derivation (for both $\kappa^2 \gtrless 0$) which were not included in the text.

The fundamental difference between the derivation for $\kappa^2 > 0$ and that for $\kappa^2 < 0$ is that when $\kappa^2 > 0$ we introduce Bloch symmetry earlier. We introduce as our unaugmented functions Bloch sums of spherical waves, i.e.,

$$\phi_{L\vec{k}}(\vec{r}) \equiv \sum_{\vec{R}} e^{+i\vec{k}\cdot\vec{R}} H_L(\vec{r}-\vec{R}) , \tag{A1}$$

where $H_L(\vec{r})$ is defined in Sec. II C. Such a Bloch sum can be rewritten using structure constants as follows

$$\phi_{L\vec{k}}(\vec{r}) = N_L(\vec{r}) + \sum_{L'} B_{LL'}(\vec{k}) J_{L'}(\vec{r}) , \tag{A2}$$

where $J_L(\vec{r})$ is defined in Eq. (10); the $B_{LL'}(\vec{k})$ are the structure constants defined in Eqs. (11), (13), and (30) and $N_L(\vec{r})$ is defined as follows:

$$N_L(\vec{r}) \equiv i^l \kappa^{l+1} n_l(\kappa r) Y_L(\hat{r}) , \tag{A3}$$

where $n_l(x)$ is a spherical Neumann function,[20]

$$h_l^+(x) = n_l(x) + i j_l(x) . \tag{A4}$$

Once the unaugmented function is expressed as in Eq. (A2), we proceed, as in Sec. II, by augmenting the functions $N_L(\vec{r})$ and $J_L(\vec{r})$. (Note that for notational simplicity the present development applies to a Bravais lattice; the extension to a lattice with a basis is straightforward.)

The second distinguishing feature of the $\kappa^2 > 0$ case is that periodicity makes the unit cell, rather than all of space, the fundamental domain of integration. Accordingly, in this appendix the notation $\langle \cdots | \cdots \rangle$ will indicate integration over the unit cell. We express matrix elements of the Hamiltonian as follows

$$\langle \tilde{\phi}_{L\vec{k}} | \mathcal{H} | \tilde{\phi}_{L'\vec{k}} \rangle = \langle \tilde{\phi}_{L\vec{k}} | \mathcal{H} | \tilde{\phi}_{L'\vec{k}} \rangle_0 + \langle \phi_{L\vec{k}} | \mathcal{H}_0 | \phi_{L'\vec{k}} \rangle' , \tag{A5}$$

where the tilde, as in Sec. II indicates augmentation; $\langle \circ\circ\circ | \circ\circ\circ \rangle_0$ indicates integration over the atomic sphere; $\langle \cdots | \cdots \rangle'$ ($\equiv \langle \circ\circ\circ | \circ\circ\circ \rangle - \langle \circ\circ\circ | \circ\circ\circ \rangle_0$) indicates integration over the interstitial region, and $\mathcal{H}_0$ is the free-particle Hamiltonian ($\mathcal{H}_0 \equiv -\nabla^2$). We now rewrite the integral over the interstitial region as an integral over the unit cell minus the integral over the atomic sphere,

$$\langle \tilde{\phi}_{L\vec{k}} | \mathcal{H} | \tilde{\phi}_{L'\vec{k}} \rangle = \langle \phi_{L\vec{k}} | \mathcal{H}_0 | \phi_{L'\vec{k}} \rangle + \{ \langle \tilde{\phi}_{L\vec{k}} | \mathcal{H} | \tilde{\phi}_{L'\vec{k}} \rangle_0 - \langle \phi_{L\vec{k}} | \mathcal{H}_0 | \phi_{L'\vec{k}} \rangle_0 \} , \tag{A6}$$

where the bracketed quantity is the augmentation correction. Using the fact that the unaugmented functions are eigenfunctions of $\mathcal{H}_0$,

$$\mathcal{H}_0 \phi_{L\vec{k}}(\vec{r}) = -\nabla^2 \phi_{L\vec{k}}(\vec{r}) = \kappa^2 \phi_{L\vec{k}}(\vec{r}) , \tag{A7}$$

we have that

$$\langle \tilde{\phi}_{L\vec{k}} | \mathcal{H} | \tilde{\phi}_{L'\vec{k}} \rangle = \kappa^2 \langle \phi_{L\vec{k}} | \phi_{L'\vec{k}} \rangle + \{ \langle \tilde{\phi}_{L\vec{k}} | \mathcal{H} | \tilde{\phi}_{L'\vec{k}} \rangle_0 - \kappa^2 \langle \phi_{L\vec{k}} | \phi_{L'\vec{k}} \rangle_0 \} . \tag{A8}$$

To evaluate the integral $\langle \phi_{L\vec{k}} | \phi_{L'\vec{k}} \rangle$ we combine Eq. (A7) with the corresponding equation for the derivative of $\phi_{L\vec{k}}(\vec{r})$ with respect to κ^2,

$$(\nabla^2 + \kappa^2) \dot{\phi}_{L\vec{k}} = -\phi_{L\vec{k}} ,$$

to obtain the following expression for the normalization integral $\langle \phi_{L\vec{k}} | \phi_{L'\vec{k}} \rangle$

$$\langle \phi_{L\vec{k}} | \phi_{L'\vec{k}} \rangle = \int d^3r \{ \dot{\phi}_{L'\vec{k}}(\vec{r}) \nabla^2 \phi^*_{L\vec{k}}(\vec{r}) - \phi^*_{L\vec{k}}(\vec{r}) \nabla^2 \dot{\phi}_{L'\vec{k}}(\vec{r}) \} \tag{A9a}$$

$$= \int d\vec{s} \cdot \{ \dot{\phi}_{L'\vec{k}}(\vec{r}) \vec{\nabla} \phi^*_{L\vec{k}}(\vec{r}) - \phi^*_{L\vec{k}}(\vec{r}) \vec{\nabla} \dot{\phi}_{L'\vec{k}}(\vec{r}) \} . \tag{A9b}$$

At the analogous point in the development in Sec. II we used the fact that on the surface at infinity enclosing all of space the spherical waves for $\kappa^2 < 0$ vanish; the corresponding fact which we exploit here is that the periodicity of $\phi_{L\vec{k}}(\vec{r})$ and $\dot{\phi}_{L\vec{k}}(\vec{r})$ cause the integral over the surface of the unit cell to vanish. The entire normalization integral is therefore equal to the integral [Eq. (A9b)] over the surface of a small sphere containing the origin.

When we write the integration over the interstitial region as the integral over the entire unit cell minus the integral over the atomic shere, we implicitly add and subtract the singular integral $\langle N_L | N_L \rangle_0$. Noting that the analysis involving Eqs. (A7) and (A9), which we have used to represent the volume integral $\langle \phi_{L\vec{k}} | \phi_{L'\vec{k}} \rangle$ as a surface integral, can equally well be applied to the integral $\langle N_L | N_L \rangle_0$, we eliminate the artifactually introduced singular integral, obtaining

$$\langle \phi_{L\vec{k}} | \phi_{L'\vec{k}} \rangle - \langle N_L | N_L \rangle_0 \delta_{LL'} = \dot{B}_{LL'}(k) + \langle N_L | N_L \rangle' \delta_{LL'} \tag{A10}$$

where $\langle N_L | N_L \rangle'$ is given by

$$\langle N_L | N_L \rangle' = -r^2 \left(\dot{m}_l(r) \frac{d}{dr} m_l(r) - m_l(r) \frac{d}{dr} \dot{m}_l(r) \right) ; \quad r = S , \tag{A11}$$

where S is the radius of the atomic sphere and $m_l(r)$ is a spherical Neumann function[20] from which the leading κ dependence has been eliminated, i.e.,

$$m_l(r) \equiv \kappa^{l+1} n_l(\kappa r) . \tag{A12}$$

Our systematic elimination of the leading κ dependence of the spherical waves [Eqs. (4), (10), and (A12)] facilitated the evaluation of the surface in-

tegral over the small sphere containing the origin, because in the limit of small r the κ^2 derivative, indicated by the dot in Eq. (A9b), acts only on the structure constant (once the singular contribution from $\langle N_L|N_L\rangle_0$ is removed). We are now essentially finished, for substitution of Eq. (A10) into our representation of the matrix element [Eq. (A8)] yields

$$\langle\tilde{\phi}_{L\vec{k}}|\mathcal{H}|\tilde{\phi}_{L'\vec{k}'}\rangle = [\epsilon_l^{(N)}\langle\tilde{N}_L|\tilde{N}_L\rangle_0 + \kappa^2\langle N_L|N_L\rangle']\delta_{LL'} + \kappa^2\dot{B}_{LL'}(\vec{k}) + B^{\dagger}_{LL'}(\vec{k})[\epsilon_{l'}^{(N)}\langle\tilde{J}_{L'}|\tilde{N}_{L'}\rangle_0 - \kappa^2\langle J_{L'}|N_{L'}\rangle_0] + [\epsilon_l^{(J)}\langle\tilde{N}_L|\tilde{J}_L\rangle_0 - \kappa^2\langle N_L|J_L\rangle_0]B_{LL'}(\vec{k}) + \sum_{L''} B^{\dagger}_{LL''}(\vec{k})[\epsilon_{l''}^{(J)}\langle J_{L''}|J_{L''}\rangle_0 - \kappa^2\langle J_{L''}|J_{L''}\rangle_0]B_{L''L'}(\vec{k}), \quad \text{(A13)}$$

where we have used the representation of $\phi_{L\vec{k}}(\vec{r})$ in terms of $J_L(\vec{r})$ and $N_L(\vec{r})$ [Eq. (A2)] to represent the integral $\langle\phi_{L\vec{k}}|\phi_{L\vec{k}}\rangle_0$. The similarity of Eq. (A13) to the result obtained in the $\kappa^2<0$ case [Eq. (29)] is clear. The overlap matrix is obtained as in Sec. IID by setting the energies appearing in Eq. (A13) (κ^2, $\epsilon_l^{(J)}$ and $\epsilon_l^{(N)}$) to unity. The Bessel-function integrals over the atomic sphere, which appear in Eq. (A13), are given by Morse and Feshbach.[30]

*Permanent address: Ruhr Universität, Abteilung für Physik, Bochum, West Germany.

[1]G. Simons, Chem. Phys. Lett. 12, 404 (1971); G. Simons and A. N. Bloch, Phys. Rev. B 7, 2754 (1973); J. St. John and A. N. Bloch, Phys. Rev. Lett. 33, 1095 (1974); E. S. Machlin, T. P. Chow, and J. C. Phillips, *ibid.* 38, 1292 (1977).

[2]J. R. Chelikowsky and J. C. Phillips, Phys. Rev. Lett. 39, 1687 (1977).

[3]R. E. Watson and L. H. Bennett (unpublished).

[4]A. Miedema, F. de Boer, and P. de Chatel, J. Phys. F 3, 1558 (1973); A. Miedema, J. Less Common Met. 32, 117 (1973); A. Miedema, J. Phys. F 3, 1803 (1973); 4, 120 (1974).

[5]J. A. Alonso and L. A. Girifalco, J. Phys. Chem. Solids 39, 79 (1978); 38, 869 (1977).

[6]V. L. Moruzzi, A. R. Williams, and J. F. Janak, Phys. Rev. B 15, 2854 (1977); J. F. Janak, V. L. Moruzzi, and A. R. Williams, Phys. Rev. B 12, 1257 (1975).

[7]P. Hohenberg and W. Kohn, Phys. Rev. 136, B 864 (1964); W. Kohn and L. J. Sham, Phys. Rev. 140, A 1133 (1965); L. Hedin and B. I. Lundqvist, J. Phys. C 4, 2064 (1971).

[8]O. K. Andersen, Phys. Rev. B 12, 3060 (1975).

[9]D. G. Pettifor, Commun. Phys. 1, 141 (1976).

[10]V. K. Ratti and J. M. Ziman, J. Phys. F 4, 1684 (1974).

[11]D. Cragg and G. Fletcher, J. Phys. F 7, 87 (1977).

[12]L. Brewer, *Phase Stability in Metals and Alloys*, edited by P. S. Rudman, J. Stringer, and R. I. Jaffee (McGraw-Hill, New York, 1967), p. 39.

[13]U. K. Poulsen, J. Kollar, and O. K. Andersen, J. Phys. F 6, L241 (1976).

[14]C. D. Gelatt, Jr., H. Ehrenreich, and R. E. Watson, Phys. Rev. B 15, 1613 (1977).

[15]D. G. Pettifor, J. Phys. F 8, 219 (1978).

[16]The canonical band idea introduced in Ref. 8 is a very powerful approximation technique, for it eliminates the necessity of performing energy-band calculations. The price for this enormous benefit is the neglect of the interaction of bands derived from atomic states of different angular-momentum character. This interaction (hybridization) appears to be relatively unimportant in many instances, but we feel it should be included in the calculation of cohesive properties. The importance of hybridization is discussed in Refs. 14 and 15.

[17]The description of changes in core states requires that the basis contain two or more orbitals for each affected core state; this is seldom the case.

[18]J. C. Slater, *The Self-Consistent Field for Molecules and Solids: Quantum Theory of Molecules and Solids* (McGraw-Hill, New York, 1974), Vol. 4; K. H. Johnson and F. C. Smith, Jr., Phys. Rev. B 5, 831 (1972).

[19]Core states can (and do) respond to changes in the valence electronic structure, but this is primarily an intra-atomic effect and therefore need not be determined as part of the interatomic problem, but rather as a self-consistent intra-atomic response to the solution of the latter.

[20]A. Messiah, *Quantum Mechanics* (North-Holland, Amsterdam, 1961), Vol. I, Appendix B.

[21]O. Gunnarsson, J. Harris, and R. O. Jones, J. Phys. C 9, 2739 (1976). The use of a single fixed value of κ is a severe approximation and only justifiable here because our spherical approximation to the intra-atomic regions eliminates, at least in an average way, the interatomic region altogether. This elimination calls attention to the fact that the spherical waves are used here in two distinct ways: (i) as a trial orbital in the interatomic region, and (ii) as a trial phase relationship among the atomic orbitals in different intra-atomic regions. (These comments, while appropriate to the portion of the text where they are referenced, require for their full appreciation the information in the balance of Sec. II.) With regard to the use of the spherical wave as a trial orbital in the interatomic region, the physical content of the single-fixed-κ approximation is that the kinetic energy of the orbital is taken to have a sin-

gle (and in general inappropriate) value over the energy range in which the particular orbital contributes to the state density. This involves an error roughly the size of the bandwidth times the fraction of the state contained in the interatomic region. The error can be reduced but not eliminated by making the κ value l and site dependent. Some measure of the severity of this problem is exhibited in Fig. 3 of Gunnarsson *et al.* which shows the variation of orbital eigenenergies with κ in a molecular calculation in which the interatomic region cannot be eliminated.

[22]N. D. Lang and A. R. Williams, Phys. Rev. Lett. 34, 531 (1975).

[23]In the traditional form of Slater's APW method each basis function is energy dependent and possesses a discontinuity in slope. The energy dependence represents another accuracy-efficiency tradeoff. When the energy dependence is eliminated, as in the Linear-Augmented-Plane-Wave method, the slope discontinuity is eliminated [see Ref. 8 and D. D. Koelling and G. O. Arbman, J. Phys. F. 5, 2041 (1975)] and the APW and ASW become conceptually very similar.

[24]In the intra-atomic region in which $H_L(\vec{r}-\vec{R})$ is centered a linear combination of radial functions is not required; only the particular solution corresponding to the designated value of l [$L \equiv (l,m)$] and the energy and normalization necessary for continuity of value and slope are required. In intra-atomic regions other than the one in which $H_L(\vec{r}-\vec{R})$ is centered a linear combination is required. The coefficients in the linear expansion are the "structure constants"; see text below.

[25]J. Korringa, Physica 13, 392 (1947); W. Kohn and N. Rostoker, Phys. Rev. 94, 1111 (1954).

[26]The augmentation procedure embodied in Eqs. (4)–(15) also eliminates the difficulty which occassionally arises in applications of the procedure of Ref. 8, when the Wronskian in the denominator of Eqs. (2.7) and (2.8) of Ref. 8 is small or vanishes. The Wronskian becomes small when the linear approximation to the energy dependence of solutions of the radial Schrödinger equation is used over too great an energy range, i.e., when the function to be synthesized possesses a logarithmic derivative more like that of the energy derivative than that of the function itself. Since the logarithmic derivatives associated with Hankel and Bessel functions differ increasingly with increasing l, the difficulty arises most frequently for large l. While this difficulty can normally be rectified, by changing the origin of the energy Taylor series for example, the automatic character of our augmentation procedure seems preferable both from the viewpoint of reliability and because it eliminates subjective choices from the study of chemical trends. The great emphasis given the linear approximation to the energy dependence of radial functions in Ref. 8 tends to identify the names LMTO and LAPW with its use. (See, e.g., Koelling and Arbman, Ref. 23.) We have chosen the name ASW for the method developed here in part because it reflects the fact that we make no use of this approximation in constructing the basis set or the secular matrix. (The principal motivation for choosing the ASW for our method is, however, our belief that the important concept in this context is augmentation, which can be used to introduce local atomic detail into plane waves, spherical waves, Gaussians, Slater functions, etc. Since our method is simply the application of this general concept to spherical waves, we feel the name ASW is uniquely appropriate.)

[27]Similar benefits are obtained within the formulation of Ref. 8 when what is called "the combined correction" is implemented; see Eqs. (4.12)–(4.20) of Ref. 8.

[28]Multiplying Eq. (28) by $H_L^*(\vec{r}-\vec{R}_\nu)$, subtracting the result from $H_{L'}(\vec{r}-\vec{R}_{\nu'})(\nabla^2+\kappa^2)H_L^*(r-\vec{R}_\nu)=0$ and integrating over all space provides a relationship between the desired integral and

$$\int d^3r\,[H_{L'}(\vec{r}-\vec{R}_{\nu'})\nabla^2 H_L^*(r-\vec{R}_\nu) - H_L^*(\vec{r}-\vec{R}_\nu)\nabla^2 H_{L'}(\vec{r}-\vec{R}_{\nu'})].$$

After integrating by parts, the latter quantity becomes an integral over small spherical surfaces containing the points of singularity ($\vec{r}=\vec{R}_\nu$ and $\vec{r}=\vec{R}_{\nu'}$). The introduction of the structure-constant expansion [Eq. (13)] permits the surface integrals to be easily evaluated, giving us Eq. (27).

[29]The required structure constants are identical to those discussed by Ham and Segall [F. S. Ham and B. Segall, Phys. Rev. 124, 1786 (1961)] and more recently by Williams *et al.* [A. R. Williams, J. F. Janak, and V. L. Moruzzi, Phys. Rev. B 6, 4509 (1972)], with one small exception; when the kinetic-energy parameter κ^2 is negative, the excluded contribution corresponding to $\vec{R}=0$ in Eq. (30) corresponds to replacing the Neumann function appearing in Eq. (18) of Ham and Segall by a Hankel function. The net result of this difference is that $D_L^{(3)}$ for $\kappa^2<0$ is given by

$$D_L^{(3)} = -2\sqrt{\eta}\left[-e^{\kappa^2/\eta}+\left(\frac{-\pi\kappa^2}{\eta}\right)^{1/2} + \frac{2\kappa^2}{\eta}\sum_{n=0}^{\infty}\frac{(\kappa^2/\eta)^n}{n!\,(2n+1)}\right]$$

(in the notation of Williams *et al.*).

[30]P. M. Morse and H. Feshbach, Methods of Theoretical Physics (McGraw-Hill, New York, 1953), Vol. II, p. 1574.

[31]The convergence of the three-center contribution [the last term in Eq. (29)] raises the issue of the energy origin to which κ^2 and the potential are referred. When the quantity $\epsilon_{l''}^{(J)}\nu''\langle\tilde{J}_{L''}|\tilde{J}_{L''}\rangle_{\nu''}-\kappa^2\langle J_{L''}|J_{L''}\rangle_{\nu''}$ is regarded as a single radial integral, it is clear that it vanishes most rapidly with increasing l'' if κ^2 is referred to the value of the effective potential at the surface of the atomic sphere. The latter is however a site-dependent quantity, whereas κ^2 is global. We therefore refer κ^2 to an average of the potentials on the individual atomic spheres, weighted by the surface area of each sphere. This energy reference is the analog in the present method of the "muffin-tin zero."

[32]P. W. Anderson, Phys. Rev. 181, 25 (1969).

[33]D. J. Chadi, Phys. Rev. B 16, 3572 (1977).

[34]Consider for a moment radial functions characterized by the energy ϵ and by their normalization for small r (e.g., $\lim_{r\to 0} R_l(r,\epsilon)=r^l$). Straightforward manipulations of the radial Schrödinger equation and its energy derivative provide the following expression for the normalization of such solution

$$N(r,\epsilon) = r^2 \left(R_l(r,\epsilon) \frac{d^2}{dr\,d\epsilon} R_l(r,\epsilon) - \frac{d}{dr} R_l(r,\epsilon) \frac{d}{d\epsilon} R_l(r,\epsilon) \right),$$

where

$$N(r,\epsilon) = \int_0^r dr_1\, r_1^2 R_l^2(r_1,\epsilon).$$

This expression for the normalization shows that energy derivatives of the normalization are proportional to the next-higher-order derivative of the radial function. In particular, since the radial functions are approximately linear over the relevant energy range (Ref. 8), the normalization is approximately constant.

[35]The normalization matrix is affected by atomic-sphere overlap and l convergence even less than the Hamiltonian matrix (See Ref. 31).

[36]We distribute $\delta^{(k)}$ among the atomic spheres according to the magnitude of the contribution to which it is added. In the calculations described in Secs. III and IV, the L summation in the three-center contribution to the secular matrix was extended to a value of l greater by one than that used in the basic ASW expansion of the wave function in that particular sphere. In these calculations the treatment of $\delta^{(k)}$ consisted, therefore, of rescaling the three-center contribution to the normalization [the fourth term in Eq. (35)] corresponding to the largest value of l used in the particular sphere. When this procedure *would* result in a negative contribution to the partial state density for a particular state, the contribution corresponding to the largest value of l is set to zero and the value for the next-largest value of l reduced.

[37]E. P. Wigner and F. Seitz, Phys. Rev. 43, 804 (1933); Solid State Phys. 1, 97 (1955).

[38]A. R. Williams and N. D. Lang, Phys. Rev. Lett. 40, 954 (1978).

[39]A. Zunger and A. J. Freeman, Phys. Rev. B 15, 4716 (1977).

[40]D. A. Liberman, Phys. Rev. B 3, 2081 (1971).

[41]J. F. Janak, Phys. Rev. B 9, 3985 (1974).

[42]Empirical evidence is provided by the fact that we have integrated the pressure to find the (negative) work required to compress the lattice from the free-atom limit to equilibrium and obtained essentially the same cohesive energy as given by the corresponding total energy difference. An alternative route to Eq. (56) is to simply regard it as an approximation to the corresponding integral over the surface of the polyhedral atomic cell; this is the argument used in Ref. 9.

[43]Determination of equilibrium by means of the pressure rather than by minimization of the total energy is not as advantageous as it might appear; the total energy, because it is a variational quantity, requires a lower degree of self-consistency to be of practical utility than does the nonvariational pressure.

[44]H. L. Skriver, O. K. Andersen, and B. Johansson, Phys. Rev. Lett. 41, 42 (1978).

[45]Core states which are not completely localized inside the atomic sphere require special treatment. The facts that the treatment should accommodate are the following: The kinetic energy of such states changes appreciably when the solid is formed and even when the crystal structure is changed. Numerical experiments using the KKR method indicate that it is not the interatomic "banding" of core levels which is important, but rather the intra-atomic response of core states to changes in the screening of the nucleus caused by intrinsically interatomic changes in the valence electron distribution. (Such changes are of three types, changes in the distribution of valence charge among s, p, d, etc. states, changes in boundary conditions resulting from bonding, and charge transfer.) Since kinetic-energy changes reflect changes in the *shape* of the core-level orbitals (as opposed to simple potential energy shifts), we are inclined not to treat core levels as "frozen" until further study demonstrates the irrelevance of core-orbital changes to binding. (All the core orbitals in the calculations described in this paper were recomputed as part of the self-consistency cycle.) Since, as mentioned, interatomic banding of the core levels does not appear to be important, we have elected to treat core levels as confined to the atomic sphere, but constructed to satisfy a boundary condition on the atomic sphere which causes their contribution to the hydrostatic pressure to vanish identically. There is a single boundary condition for each core state which affects this. Since cohesion can be thought of as integration of the hydrostatic pressure, this treatment of the core eliminates any direct contribution of the core to bonding and cohesion; the essential role that changes in the core kinetic energy play in satisfying the virial theorem indicate an indirect role. The role of core electrons in metallic bonding has been studied by Janak [J. F. Janak, Solid State Commun., 20, 151 (1976)] for the case of simple metals.

[46]O. Gunnarsson, J. Harris, and R. O. Jones, J. Chem. Phys. 67, 3970 (1977).

[47]N. D. Lang, Solid State Phys. 28, 225 (1973).

[48]In other words, analysis of cohesion in terms of the the one-electron energies ignores (among other things) proton potential-energy changes.

[49]On forming a $3d$-transition metal, e.g., from free atoms, the d electrons move away from the nucleus by a small amount and their kinetic energy decreases. This outward displacement reduces the screening of the nucleus for the $3p$ electrons, causing them to sink deeper into the core with increased kinetic energy, thereby satisfying the virial theorem.

[50]We are indebted to U. von Barth for this analysis of T_{xc} and its role in the virial theorem.

[51]By empty lattice we mean-free space viewed as a periodic array of potentials which do not scatter electrons. The eigensolutions are therefore planewaves $e^{+i(\vec{k}+\vec{K})\cdot\vec{r}}$, where $\vec{k}$ is a vector in the Brillouin zone and $\vec{K}$ is a reciprocal lattice vector, and the eigenenergies are simply $|\vec{k}+\vec{K}|^2$.

[52]Note that the three-center contributions to both the Hamiltonian and overlap matrices vanish identically for the empty lattice. The question of the maximum value of L'' to which the spherical-harmonic expansion of this term in Eq. (29) must be carried does not arise.

[53]We have studied the sensitivity of both orbital and total energies to the variation of κ. The approximate elimination of the interatomic region renders the orbital energies somewhat less sensitive than those displayed by Gunnarsson *et al.*, in Ref. 21. The total energy changes by approximately 5% of the change in κ^2 over the range we have studied ($-0.1 < \kappa^2 < 0.2$). Note

that. while this variation enters directly as an error into our estimates of cohesive energies, it tends to subtract out of our estimates of heats of formation of intermetallic compounds.

[54]V. L. Moruzzi, J. F. Janak and A. R. Williams, *Calculated Electronic Properties of Metals* (Pergamon, New York, 1978).

[55]In the KKR calculations of Ref. 54 to which we compare ASW results in this section all angular momenta with $l \leq 4$ were treated equivalently.

[56]The lattice constant used is the equilibrium lattice constant given by the KKR calculations of Ref. 54; that given by the ASW calculations is essentially the same (see Table II).

[57]The source of the arbitrariness is the lattice summations required for the solution of Poisson's equation. The value of the average electrostatic potential in the unit cell depends on the order in which two limits are taken; the screening of the Coulomb interaction is allowed to vanish and the volume of the system is allowed to increase without limit. Since nothing of physical interest depends on the average potential, the arbitrariness is of no consequence. The same point is made in more physical terms by saying that there is nothing in a self-consistent energy-band calculation which indicates the magnitude of the surface dipole-layer potential; the band energies cannot, therefore, be related to vacuum.

[58]The free-atom total energies required for the specification of the cohesive energy are those given by the spin-polarized calculations of Ref. 6 and 54.

[59]Equilibrium lattice constants were obtained from the *American Institute of Physics Handbook*, 3rd ed. (McGraw-Hill, New York, 1972), Table 9d-3. Cohesive energies were obtained from L. Brewer, LBL Report No. 3720 (1975) (unpublished).

[60]Bulk moduli were obtained from O. L. Anderson, *Physical Acoustics*, edited by W. P. Mason (Academic Press, New York, 1965), Vol. III-B, pp. 77–95.

[61]We associate with the word "covalent" the strong interaction of states on different atoms, in this case the d states of Ni and p states of Al. Such interactions contribute significantly to cohesion when non- and/or antibonding hybrid orbitals resulting from the interaction are not occupied. A detailed decomposition and analysis of representative covalent bond is given by Lang and Williams [N. D. Lang and A. R. Williams Phys. Rev. B 18, 616 (1978)].

[62]See, e.g., V. L. Moruzzi, A. R. Williams, and J. F. Janak, Phys. Rev. B 10, 4856 (1974); A. Neckel, P. Rastl, R. Eibler, P. Weinberger, and K. Schwartz, J. Phys. C 9, 579 (1976); A. Zunger and A. J. Freeman, Phys. Rev. B 16, 906 (1978).

[63]With regard to the stability of our calculations with respect to the expansion of one atomic sphere at the expense of another at constant total volume, it is not clear that the calculations are stable, *in principle*. One implication of the assumption of spherical symmetry (of the electron density and effective potential) is that the electrostatic potential is continuous for only a single value of the relative sphere sizes. For the case of two atoms per unit cell, the local Hartree potential equals $+2\delta q/S_1$ on sphere "1" and $-2\delta q/S_2$ on sphere "2". (δq is the deviation from neutrality.) The Madelung potential [Eq. (52)] acts to eliminate this discontinuity, but, since it is independent of the sphere radii S_1 and S_2, it can do so only for a unique value of the S_1/S_2. By equating the discontinuity $2\delta q(S_1^{-1} - S_2^{-1})$ to the site difference of the Madelung potential $\phi_2^M - \phi_1^M$ [Eq. (52)] we can solve for the unique radius ratio appropriate to a given lattice structure. [Note that, since both ϕ_ν^M and the discontinuity $2\delta q(S_1^{-1} - S_2^{-1})$ are linear in δq, the result is independent of δq]. The resulting radius ratio for the CsCl structure of 0.94 and for the NaCl structure it is 0.66. Using spatial decompositions other than those corresponding to these special radii ratios creates discontinuities which the self-consistent field process cannot screen by means of charge transfer. The correct interpretation of calculations done for other radii ratios is not clear; it is fortunate therefore that deviations from the theoretically justifiable radii ratios, empirically, have little effect on the calculations. The one exception to the last statement which we have encountered is the case of NaCl, for which the partitioning of space consistent with the intuitive picture of a large negative chlorine ion and a small positive sodium ion is inconsistent with the relative sizes of the two atomic cores. We found that the total energy was, however, stable when NaCl was taken to have the CsCl structure. Since the Madelung energies of the two structures are extremely similar, we think the results obtained using the CsCl structure constitute a reliable estimate of those appropriate to the real material and it is these which are given in Table III. We feel that the greatest cancellation of systematic errors is achieved in our calculations by using the ratio corresponding to the equilibrium volumes of the elemental constituents. Thus, for example, in systems for which the volume of the compound equals the sum of the elemental volumes (Vegard's Law), the calculated heat of formation results exclusively from boundary-condition changes and charge transfer. The results shown in Table III for NiAl and CuZn were obtained using this strategy. The results for NaCl and the hydrides were obtained using the radius ratio for which the electrostatic potential is continuous.

[64]By "binding energy of interest" we mean the total energy relative to that of separated ions in the case of NaCl and to that of the pure metal constituents in the case of CuZn and NiAl. Note that, when defined this way, CuZn is a weakly bound system. This does not mean that CuZn can be easily separated into free atoms (the cohesive energies of pure Cu and pure Zn are appreciable, ~ 3 eV/atom), but it does mean that with our calculations we are pursuing a rather subtle effect.

[65]C. Kittel, *Introduction to Solid State Physics*, 5th ed. (Wiley, New York, 1976), Table 6.

[66]W. B. Pearson, *A Handbook of Lattice Spacings of Metals and Alloys* (Pergamon, New York, 1967), Vol. 2.

[67]R. Hultgren, P. D. Desai, D. T. Hawkins, M. Gleiser, and K. K. Kelly, *Selected Values of the Thermodynamic Properties of Binary Alloys* (Am. Soc. for Metals, Metals Park, Ohio, 1973).

[68]A. C. Switendick, in *Topics in Applied Physics*, edited by G. Alefeld and J. Völkl (Springer-Verlag, Heidelberg, 1978), Vol. 28, Chap. 5.

[69]C. D. Gelatt, Jr., H. Ehrenreich, and J. A. Weiss, Phys. Rev. B 17, 1940 (1978); C. D. Gelatt, Jr., J. A. Weiss, and H. Ehrenreich, Solid State Comm. 17, 663

(1975).

[70]As in the discussion of Sec. II F the energy origin appropriate to the present discussion is the zero of the local Hartree potential. This can be seen as follows: A neutral hydrogen atom is brought through the dipole layer potential without energy cost or benefit. In the interstitial region the proton experiences no potential energy shift due to the electrostatic potential of the neutral atoms (the local Hartree potential). It is the Fermi level referred to the potential energy of the proton which enters the energy of hydride formation.

[71]L. Hodges, R. E. Watson, and H. Ehrenreich, Phys. Rev. B 5, 3953 (1972).

[72]The basic idea here is that the added electrons simply fill the bands of the host metal to a new (higher) Fermi level, (ϵ_f), i.e., rigid-band theory. In actuality, distortions of metal bands by the hydrogenic protons account for about half the required additional states below ϵ_f. (See Refs. 68 and 69.) Approximately half the additional electrons are nonetheless accommodated by a rigid-band-like shift of ϵ_f.

[73]Note that the errors in the calculations tend to be systematic rather than random. The calculations can therefore be justifiably used to study *variations* such as those considered here which are smaller than the absolute errors in the calculation.

[74]Note that the crucial role played in our analysis by the rigid-band shift (See Ref. 72) of the chemical potential in the noble metals implies that the heat of solution in the noble metals may be strongly concentration dependent.

[75]Experimental information pertaining to NiH and PdH was obtained from W. M. Mueller, J. P. Blackledge, and G. G. Libowitz, *Metal Hydrides* (Academic, New York, 1968), Chap. 12. Lattice constants: $NiH_{0.7}$ (3.71–3.735 Å), $PdH_{0.6}$ (4.026 Å), $PdH_{0.8}$ (4.08 Å).

[76]R. B. McLellan and W. A. Oates, Acta Metall. 21, 181 (1973).

[77]The direct subtraction of the total energy of the transition metal $E(M)$ and half that of the H_2 molecule $E(H_2)$ from that of the hydride $E(MH)$ clearly involves a large loss of numerical significance. In this context we must be concerned even with the fact that the electron-gas data used to construct the exchange correlation potential was parametrized slightly differently by Gunnarsson and Lundqvist [O. Gunnarsson and B. I. Lundqvist, Phys. Rev. B 13, 4274 (1976)] for their study of the H_2 molecule. In the evaluation of the heat of hydride formation, $\Delta \equiv E(MH) - E(M) - \frac{1}{2}E(H_2)$, we have therefore represented $E(H_2)$ by $2E(H) + \delta$, where $E(H)$ is the total energy of the spin-polarized hydrogen atom given in Ref. 54 and δ is the binding energy of H_2 given by Gunnarsson and Lundqvist.